Phylogenies of Central Element Proteins Reveal the Dynamic Evolutionary History of the Mammalian Synaptonemal Complex: Ancient and Recent Components

Johanna Fraune,* Céline Brochier-Armanet,† Manfred Alsheimer,* and Ricardo Benavente*,[1]

*Department of Cell and Developmental Biology, Biocenter, University of Würzburg, Würzburg 97074, Germany, and †Laboratoire de Biométrie et Biologie Evolutive, Centre National de la Recherche Scientifique, Unité Mixte de Recherche 5558, Université Lyon 1, F-69622 Villeurbanne, France

ABSTRACT During meiosis, the stable pairing of the homologous chromosomes is mediated by the assembly of the synaptonemal complex (SC). Its tripartite structure is well conserved in *Metazoa* and consists of two lateral elements (LEs) and a central region (CR) that in turn is formed by several transverse filaments (TFs) and a central element (CE). In a previous article, we have shown that not only the structure, but also the major structural proteins SYCP1 (TFs) and SYCP3 (LEs) of the mammalian SC are conserved in metazoan evolution. In continuation of this work, we now investigated the evolution of the mammalian CE-specific proteins using phylogenetic and biochemical/cytological approaches. In analogy to the observations made for SYCP1 and SYCP3, we did not detect homologs of the mammalian CE proteins in insects or nematodes, but in several other metazoan clades. We were able to identify homologs of three mammalian CE proteins in several vertebrate and invertebrate species, for two of these proteins down to the basal-branching phylum of *Cnidaria*. Our approaches indicate that the SC arose only once, but evolved dynamically during diversification of *Metazoa*. Certain proteins appear to be ancient in animals, but successive addition of further components as well as protein loss and/or replacements have also taken place in some lineages.

SEXUAL reproduction was established as the beneficial mode of propagation during evolution of animals. Most of the metazoan species reproduce sexually meaning via formation of a new organism by syngamy, that is the fusion of two gametes from different genders. The formation of the gametes, in turn, is dependent on meiosis, a specialized type of cell division that is responsible for the reduction of the chromosome set from the original diploid state of the gonia to the haploid state of differentiated sperms or eggs. During the meiotic cell cycle, a germ cell progenitor passes through two successive rounds of chromosome segregation (called meiosis I and II) after a single round of DNA replication. In the most crucial process of meiosis I, the homologous chromosomes have to pair and exchange genetic material (homologous recombination) as a requirement for their accurate segregation into two daughter cells. An important feature of this evolutionarily well-conserved pairing process is the assembly of the synaptonemal complex (SC), a proteinaceous structure that connects the two chromosomes of a homologous pair like a zipper during prophase of meiosis I (synapsis). The successful synapsis of the chromosomes is essential for proper homologous recombination in mammals, preventing missegregation of the chromosomes that results in aneuploid germ cells or even cell death (for reviews, see Hassold and Hunt 2001; Page and Hawley 2004; Costa and Cooke 2007; Handel and Schimenti 2010; Bolcun-Filas and Schimenti 2012). Electron microscopic data of animals from several different phyla illustrated the nearly ubiquitous existence of the SC in meiosis and the evolutionary conservation of its tripartite structure (for reviews, see Gillies 1975; von Wettstein *et al.* 1984; Page and Hawley 2004). With the shape similar to that of a ladder, the SC consists of two parallel rod-like lateral elements (LEs) that are linked during

doi: 10.1534/genetics.113.156679
Manuscript received June 26, 2013; accepted for publication September 3, 2013
Supporting information is available online at http://www.genetics.org/lookup/suppl/doi:10.1534/genetics.113.156679/-/DC1.
[1]Corresponding author: Department of Cell and Developmental Biology, Biocenter, University of Würzburg, Am Hubland, 97074 Würzburg, Germany. E-mail: benavente@biozentrum.uni-wuerzburg.de

synapsis by transverse filaments (TFs) that are arranged in a crosswise fashion. The TFs from opposing LEs overlap in the center of the SC, thereby forming the central element (CE). Together, the TFs and the CE constitute the central region (CR) of the SC (for review, see Page and Hawley 2004).

In mammals, seven different SC protein components have been identified so far (for review, see Fraune *et al.* 2012a) that are essential for the correct assembly of the SC. The LEs are composed of the proteins SYCP2 and SYCP3 [1500 and 254 amino acids (aa) in mouse, respectively] (Lammers *et al.* 1994; Offenberg *et al.* 1998). Dimers of the large coiled coil protein SYCP1 (993 aa in the mouse) form the TFs (Meuwissen *et al.* 1992). In addition, four rather small proteins locate specifically to the CE: SYCE1, SYCE2, SYCE3, and Tex12 (329, 171, 88, and 123 aa in mouse, respectively) (Costa *et al.* 2005; Hamer *et al.* 2006; Schramm *et al.* 2011). These CE proteins are essential for initiation and elongation of the synapsis. A complex made of SYCE1 and SYCE3 is postulated to initiate synapsis by allowing the initial interaction of opposing TFs (Bolcun-Filas *et al.* 2007; Schramm *et al.* 2011). Both proteins localize in a continuous pattern along the SC, similar to SYCP1 (Costa *et al.* 2005; Schramm *et al.* 2011). Disruption of either SYCE1 or SYCE3 leads to a complete disruption of synapsis (Bolcun-Filas *et al.* 2009; Schramm *et al.* 2011). In contrast, SYCE2 and Tex12 present a rather punctate localization pattern and the corresponding knockout spermatocytes still exhibit short stretches of CE-like structures during the meiotic prophase I substages of zygotene and pachytene (Costa *et al.* 2005; Hamer *et al.* 2006, 2008; Bolcun-Filas *et al.* 2007). SYCE2 and Tex12 are therefore proposed to be essential for elongation of synapsis (Bolcun-Filas *et al.* 2007; Hamer *et al.* 2008).

Recently, we have shown that the main structural SC components SYCP1 (TFs) and SYCP3 (LEs) of the mouse are ancient in *Metazoa* and present in a variety of different organisms, even in the early-branching *Hydra* lineage (*Cnidaria*) (Fraune *et al.* 2012b). This opened the possibility that the entire SC could be of ancient origin, meaning that not only the main structural components of the LEs and TFs, but also the CE components of the mammalian SC might have been present in the last ancestor of metazoans. To test this hypothesis, we analyzed the evolutionary history of the mouse CE through a phylogenetic approach. We identified homologs of three of the four CE proteins in various species that belong to metazoan lineages, which are distantly related to mammals. This points to a very ancient origin of the corresponding components in *Metazoa*. More precisely, we show that SYCE2 and Tex12 were present in the ancestor of *Eumetazoa*. In contrast, the phylogeny of SYCE1 indicates that this protein is slightly more recent and emerged in the ancestor of *Bilateria*, whereas SYCE3 emerged much later in the vertebrate lineage. The two candidate components SYCE2 and Tex12 found in the cnidarian *Hydra* were analyzed experimentally to confirm their potential role in the assembly of the SC in this basal early-diverging animal lineage.

Materials and Methods

Dataset assembly

We used the four characterized mouse CE proteins SYCE1 (RefSeq: NP_001137237), SYCE2 (RefSeq: NP_082230), SYCE3 (RefSeq: NP_001156352), and Tex12 (RefSeq: NP_079963); CONA (RefSeq: NP_650719), a CR protein described in *Drosophila melanogaster*; and the *Caenorhabditis elegans* CR proteins SYP-2, SYP-3, and SYP-4 (RefSeq: NP_504462, NP_492345, and NP_491960) as seeds to query public sequence databases. Homologous sequences available in the *nr* database at the National Center for Biotechnology Information (NCBI) (http://blast.ncbi.nlm.nih.gov) were identified using the BLASTp program (Matrix: BLOSUM45; default values for all other parameters; Altschul *et al.* 1997). To ensure that all homologs were correctly sampled, we used the PSI-BLAST program (Matrix: BLOSUM45; default values for all other parameters; Altschul *et al.* 1997). Convergence was reached after three iterations. Additional or more divergent homologs were retrieved from the *nr/nt*, *est*, *wgs*, and ongoing genome projects data available at the NCBI, Ensembl database, release 71 (http://www.ensembl.org/index.html), the Dana-Farber Cancer Institute (DFCI) (http://compbio.dfci.harvard.edu), and the InParanoid 7 project (http://inparanoid.sbc.su.se/cgi-bin/index.cgi; Ostlund *et al*. 2010) using tBLASTn and BLASTp. All BLASTp and tBLASTn searches were repeated several times by using each newly detected homolog as seed for a new search. The absence of any homologous sequence in a given species/lineage, for which the complete genome is available, was checked by screening the corresponding genome with the tBLASTn program. The sequences retrieved were used for reciprocal BLAST analyses to ensure that they represented putative homologs of CE proteins (and not false positives).

For each CE protein, the retrieved sequences were aligned using ClustalO (Sievers *et al.* 2011) implemented in the Seaview program, version 4.4.0 (Gouy *et al.* 2010). A preliminary neighbor-joining (NJ) tree was inferred with the same program (default parameters). Based on this tree, the closest homologs of the sequences that were experimentally demonstrated as part of the SC (*e.g.*, the mouse sequences) were selected, realigned, and used to build a specific hidden Markov model (HMM) profile using the HMMer 3.0 webserver (http://hmmer.janelia.org). The resulting profile was used to query the *nr* database (*hmmsearch* option) as well as to individually verify all the other sequences present in the initial alignment by starting from the closest and progressing to the more distantly related sequences (according to the NJ tree). New and verified sequences were added to the new alignment step by step and used to update the HMM profile. This procedure was repeated iteratively until no further

homologs could be identified (Supporting Information, Table S1, Table S2, Table S3, and Table S4).

Phylogenetic analysis

To reduce potential tree reconstruction artifacts linked to the overrepresentation of a few lineages (such as placental mammals), a taxonomically balanced subset of homologs was selected for final phylogenetic analyses. The sequences were aligned using MAFFT version 7 with the *linsi* option, which allows accurate alignment reconstructions (Katoh *et al.* 2002). Alignments were inspected using Seaview (Gouy *et al.* 2010) and ambiguously aligned regions were removed with the Block Mapping and Gathering with Entropy (BMGE, default parameters; Criscuolo and Gribaldo 2010). Maximum likelihood (ML) trees were inferred with PhyML version 3.0.1 (Guindon *et al.* 2010) with the LG model (Le and Gascuel 2008), option NNI+SPR and a gamma distribution to take into account heterogeneous evolutionary rates (four categories of sites and an estimated alpha parameter) as suggested by the proposed model tool implemented in TreeFinder, version 2011 (aicc criterion; Jobb *et al.* 2004). The robustness of the resulting tree was assessed with the nonparametric bootstrap procedure implemented in PhyML (100 replicates of the original alignment). Bayesian phylogenetic trees (Bayesian inference, BI) were constructed using MrBayes 3.2.1 (Ronquist *et al.* 2012) with a mixed amino-acid-substitution model and gamma distribution (four categories of sites and an estimated alpha parameter). The search was run with four independent chains for 1 million generations. Trees were sampled every 100 generations. The first 2000 trees were discarded as "burn-in." The branch robustness was estimated by calculation of posterior probabilities.

Annotated sequence alignments were designed using CHROMA version 1.0 (Goodstadt and Ponting 2001). The identity threshold for grouping of the residues was set to 60%. Seven groups were created, depending on different features of the amino acids: identical, charged, Ser/Thr, aliphatic, aromatic, polar, and hydrophobic. Sparse regions longer than four residues were removed if at least 80% of the sequences were blank gaps at these positions. The number of removed residues is indicated by numbers in parentheses in the corresponding sequences at those positions (Figure 1, Figure 2, Figure S1, and Figure S2).

Animal strains and culture conditions

For expression analysis, animals from the strain *AEP* (Martin *et al.* 1997), belonging to the *Hydra vulgaris* group, were cultured at 18° following standard procedure. Induction of testes formation was achieved by feeding the animals daily for at least 1 week and starving them afterward (Wittlieb *et al.* 2006).

Sequence information of *H. vulgaris AEP* was obtained from transcriptome data on the Compagen_NG server (Hemmrich *et al.* 2012).

Isolation of RNA, reverse transcription, PCR, and cloning of cDNA

RNA extraction from whole animals or tissues of *Hydra AEP* was accomplished using the peqGOLD TriFast RNA Extraction kit (peqLab, Erlangen). cDNA was obtained by reverse transcription of 1 μg RNA with an oligo(dT) primer and M-MLV reverse transcriptase (Promega, Mannheim, Germany) and used as template for cloning of full-length cDNA sequences or expression analysis in different tissue fractions (head, midpiece, foot, and testis). Full-length cDNA of *HySyce2* and *HyTex12* was amplified with Phusion DNA polymerase (Thermo Scientific, St. Leon Roth, Germany) and the following sequence-specific primer pairs: Hy_Syce2_ATG 5′ (ATGACTAACAAACGCAAGTTTGTGAG), Hy_Syce2_TGA 3′ (CTACTGCAATGATGGATAGGTAGCTTG) at 66° and HyTex12 5′ (CTGAACATGTGTAAAAATGTCTCAG), HyTex12 3′ (CAGTT TTAATATTTAACTGTTAAAA-GTGTTAATAG) at 61°. Subsequently, the cDNA was cloned into the pSC-B-amp/kan PCR cloning Vector (Agilent Technologies, Böblingen, Germany) and sequenced. Comparison of different independent cloning attempts with sequence data on the public databases was performed to verify the obtained cDNA sequences from single-read sequencing.

Tissue-specific expression profiles of *HySyce2* and *HyTex12* were likewise analyzed by Phusion PCR using the same primer pairs. Actin expression was traced as an internal loading control with actin-specific primers (Hym_actin 5′: 5′-AAGCTCTTCCCTTGAGAAATC-3′; Hym_actin 3′: 5′-CCAAAATAGATCCTCCGATCC-3′, at 60°).

Antibodies

HySYCE2 and HyTex12 antibodies were generated against the full-length HySYCE2 and HyTex12. The proteins were expressed as His-tagged fusion proteins from the pET21a vector (Novagen, Darmstadt, Germany) and purified through a Nickel-nitrilotriacetic acid (Ni-NTA) agarose matrix (Qiagen, Hilden, Germany). Immunization of a rabbit and a guinea pig was performed by Seqlab (Göttingen, Germany). The obtained antisera of the final bleedings were affinity purified through the HiTrap system (GE Healthcare, Munich), following the manufacturer's protocol. An α-actin antibody (A4700) was purchased from Sigma (Steinheim, Germany).

SDS–PAGE and immunoblot analysis

Protein fractions from different tissues of *Hydra* (head, midpiece, foot, and testis) were separated in a 15% (vol/vol) acrylamide SDS–PAGE and subsequently transferred to nitrocellulose membranes by the semi-dry Western blotting system (Matsudaira 1987). Detection of the proteins HySYCE2 and actin was performed as previously described (Fraune *et al.* 2012b). We used a rabbit α-HySYCE2 (1:2000) that recognized a protein in the testis tissue that matches the expected molecular weight of HySYCE2 (17.6 kDa) and a mouse α-actin antibody (1:10,000) that, according to the manufacturer, has a broad species reactivity. A peroxidase-conjugated secondary antibody (1:10,000) of Dianova (Hamburg) was applied for

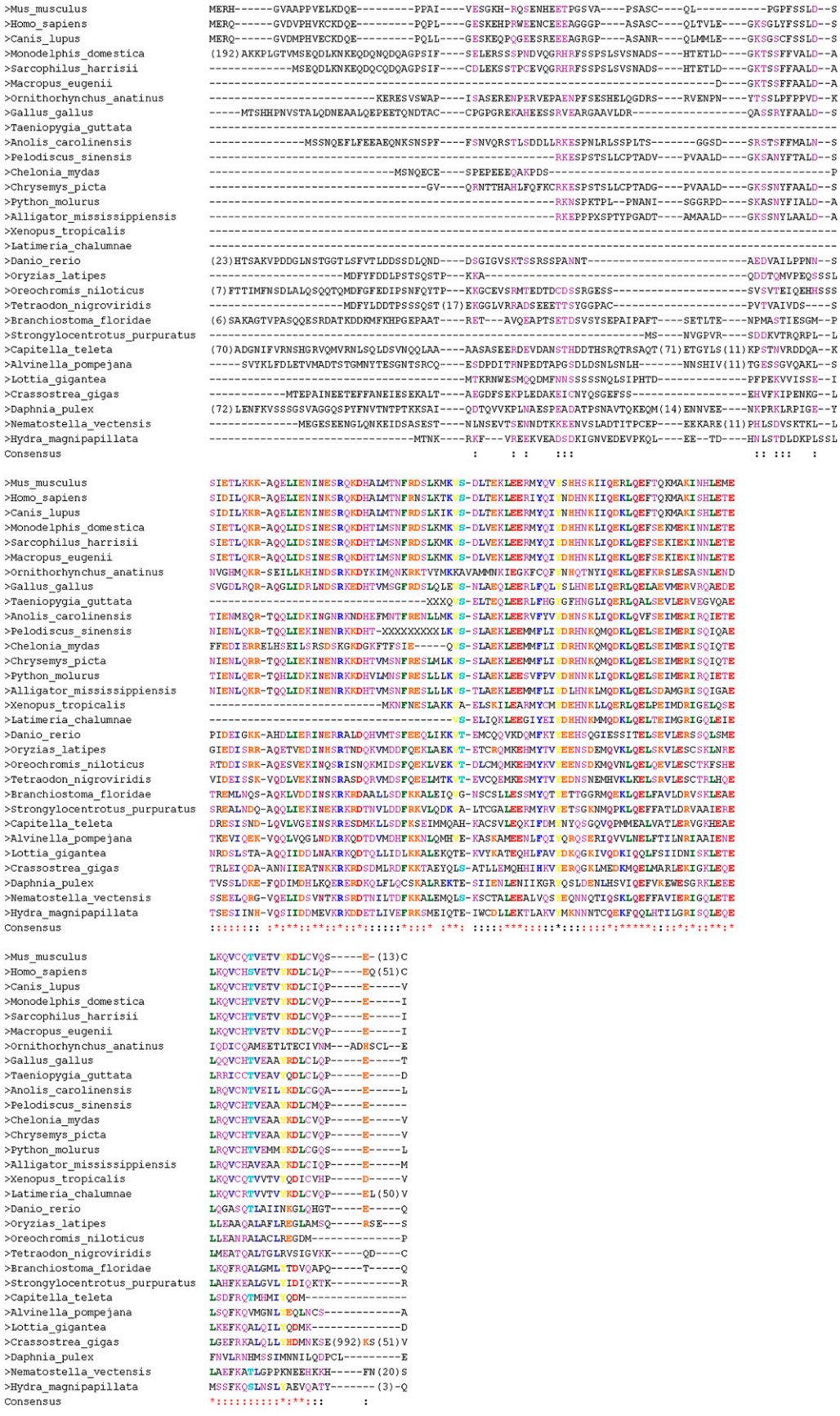

Figure 1 Multiple alignment of SYCE2 homologs. Positions kept for phylogenetic inferences are indicated in red. Positions removed by BMGE are indicated in black.

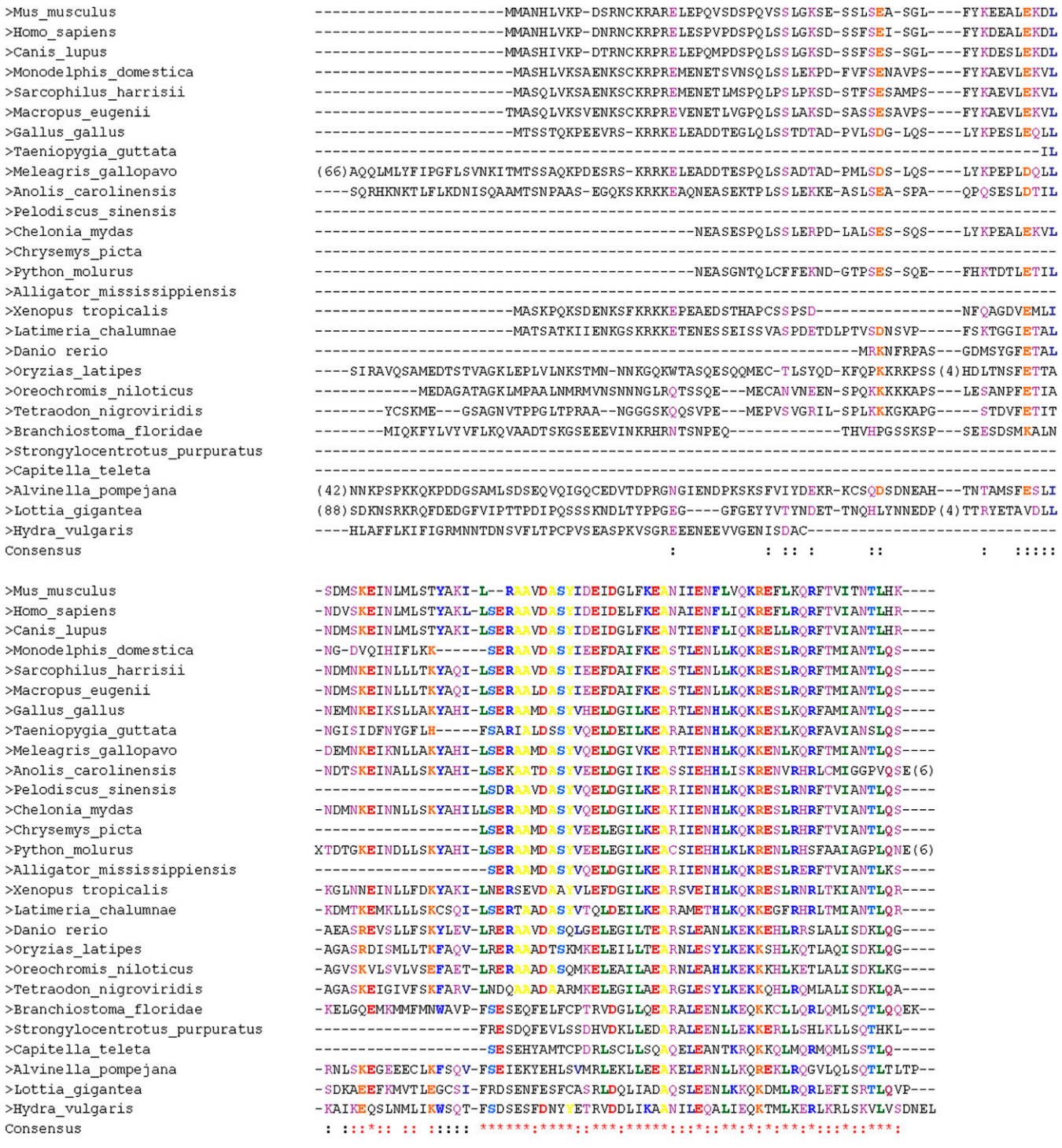

Figure 2 Multiple alignment of Tex12 homologs. Positions kept for phylogenetic inferences are indicated in red. Positions removed by BMGE are indicated in black.

final detection of the protein with the Western Lightning *Plus*-ECL (PerkinElmer, Waltham, MA). The α-HyTex12 antibody was not effective in Western blot analysis but it recognized its target protein on chromosome spreads.

In situ hybridization

Whole-mount *in situ* hybridization on *Hydra* was conducted following the standard protocol (Grens *et al.* 1996) with minor modification as reported recently (Fraune *et al.* 2012b). Digoxigenin (DIG)-labeled RNA probes were synthesized from the full-length cDNA of *HySyce2* (459 bp) and *HyTex12* (336 bp).

Immunocytochemistry

Meiotic chromosome spreads were prepared following the dry-down procedure (De Boer *et al.* 2009), but with slight

adaptions to the *Hydra* tissue (Fraune *et al.* 2012b). Immunostaining of the chromosome spreads was carried out as indicated in De Boer *et al.* (2009) with the help of following affinity-purified antibodies: rabbit α-HySYCE2 (1:200), rabbit α-HyTex12 (1:300), guinea pig α-HyTex12 (1:300), guinea pig α-HySYCP1 (1:300), rabbit α-HySYCP1 (1:900), guinea pig α-HySYCP3 (1:75), and rabbit α-HySYCP3 (1:600). Secondary antibodies were purchased from Dianova and applied as recommended by the manufacturer.

Microscopy and imaging

A Leica TCS-SP2 confocal laser scanning microscope (Leica, Wetzlar, Germany) equipped with a ×63/1.40 HCX PL APO lbd.BL oil immersion objective was used for confocal imaging. The images are 2D projections from a series of ~20 optical sections per cell, generated by the maximum projection algorithm (Leica), and they were pseudocolored using the Leica TCS-SP2 software. Processing of the digital images was done with Adobe Photoshop CS5 (Adobe Systems).

Results

Mouse CE proteins SYCE1, SYCE2, and TEX12 are ancient in Metazoa

Our in-depth survey of sequence databases revealed many homologs of the mouse SYCE1, SYCE2, and Tex12 components in representatives of distantly related animal lineages. More precisely, homologs could be identified in most *Bilateria* lineages, namely in *Chordata* (vertebrates and *Cephalochordata*) and the invertebrate lineage of *Echinodermata*, all belonging to *Deuterostomia* as well as in *Lophotrochozoa* (*Mollusca* and *Annelida*) (Table S1, Table S2, and Table S3). Conversely, we could not identify SYCE1 homologs in any bird species, although complete genome sequences are available for this lineage. This reflects either the loss or the nonhomologous replacement or a faster evolutionary rate (beyond recognition) of the SYCE1 components in this lineage. Interestingly, we also detected SYCE2 and Tex12, but not SYCE1 homologs in representatives of the basal-branching phylum of *Cnidaria*, namely *Hydra* and/or *Nematostella*, and a SYCE2 divergent homolog in the crustacean species *Daphnia pulex* (*Ecdysozoa)*. The situation was different for the last CE component, because we detected SYCE3 homologs only in vertebrate species (Table S4) despite an intense search in nonvertebrate sequence data.

The multiple alignments show that the central regions of SYCE2 (aa 59–153 of the mouse; aa 67–161 of the human) and Tex12 (aa 61–121 of the mouse; aa 61–123 of the human) are relatively well conserved across metazoans, whereas their N- and C termini are highly variable (Figure 1 and Figure 2). In contrast, SYCE1 harbors a larger conserved region that corresponds to a large part of the central coiled coil domain of the protein (aa 58–268 of the mouse; aa 56–266 of the human; Figure S1). The ML and BI phylogenies of SYCE2 and Tex12 are not fully resolved, especially for the deepest nodes [weak bootstrap values (BVs) and Bayesian posterior probabilities (PPs] (Figure 3, A and B). This is not surprising, given the relatively restricted number of positions that have been kept for phylogenetic analyses (Figure 1 and Figure 2) and the relatively long branches associated to some invertebrate species (*i.e.*, *D. pulex*, Figure 3A or *Alvinella pompejana* and *Capitella teleta*, Figure 3B), indicating fast evolutionary rates. The recovered relationships among vertebrate lineages, however, are globally consistent with recently published phylogenies (Philippe *et al.* 2009; Simakov *et al.* 2013). In the case of SYCE1, more positions could be kept for the phylogenetic analysis (Figure S1) and, unsurprisingly, the resulting ML and BI trees are more resolved (Figure 3C) and consistent with the global phylogeny of *Metazoa*. Finally, the ML and BI trees of SYCE3 (based on the conserved region of aa 1–86 of the mouse and the human; Figure S2) are globally consistent with the phylogeny of vertebrates (Figure 3D), suggesting that this component emerged in the ancestor of this lineage.

The presence of homologs of SYCE2, Tex12, and SYCE1 in most bilaterian lineages was suspected, as we had previously proved the ancient and monophyletic origin of the two *bona fide* structural SC components SYCP1 and SYCP3 (Fraune *et al.* 2012b). Indeed, our data suggest that these three CE components were likewise present in the last common ancestor of *Bilateria*. The origin of SYCE2 and Tex12 can even be pushed back to the ancestor of *Eumetazoa*, given that homologs of these two components have been detected in *Cnidaria* representatives. At this step, a more ancient origin, however, cannot be proposed, because (despite many attempts) we neither detected homologs of these two components in *Porifera* or in *Placozoa* (two basal-branching metazoan lineages) nor in protist lineages closely related to *Metazoa* (*i.e.*, *Choanoflagellida*, *Ichthyosporea*, etc.) for which complete genome sequences are available. In contrast, SYCE3 seems to be of much more recent origin, likely being an innovation of vertebrates.

Despite our extensive survey of sequence databases, we did not detect any homolog of the mammalian CE components in ecdysozoan species, including *D. melanogaster* and *C. elegans*. Instead, alternative CR proteins that do not share any sequence homology with other proteins were characterized in these model organisms for meiosis (MacQueen *et al.* 2002; Colaiacovo *et al.* 2003; Smolikov *et al.* 2007, 2009; Page *et al.* 2008; Schild-Prüfert *et al.* 2011). As the single exception to the remarkable situation of the ecdysozoan lineage, we identified a potential homolog of SYCE2 in the *Crustacea D. pulex*. Regarding its very long branch in the SYCE2 phylogenetic tree (Figure 3A), the evolutionary distance between this protein and the other SYCE2 sequences, however, seems to be peculiarly large and suggests a fast evolutionary rate.

In *D. melanogaster*, the Corona (CONA) protein seems to stabilize the interaction of the TFs in the center of the SC, which is comparable to the function of the mammalian SYCE2/Tex12 complex (Page *et al.* 2008). Besides C(3)G, it is the only identified CR protein in *D. melanogaster* so far. According to the authors' own statement, CONA is only

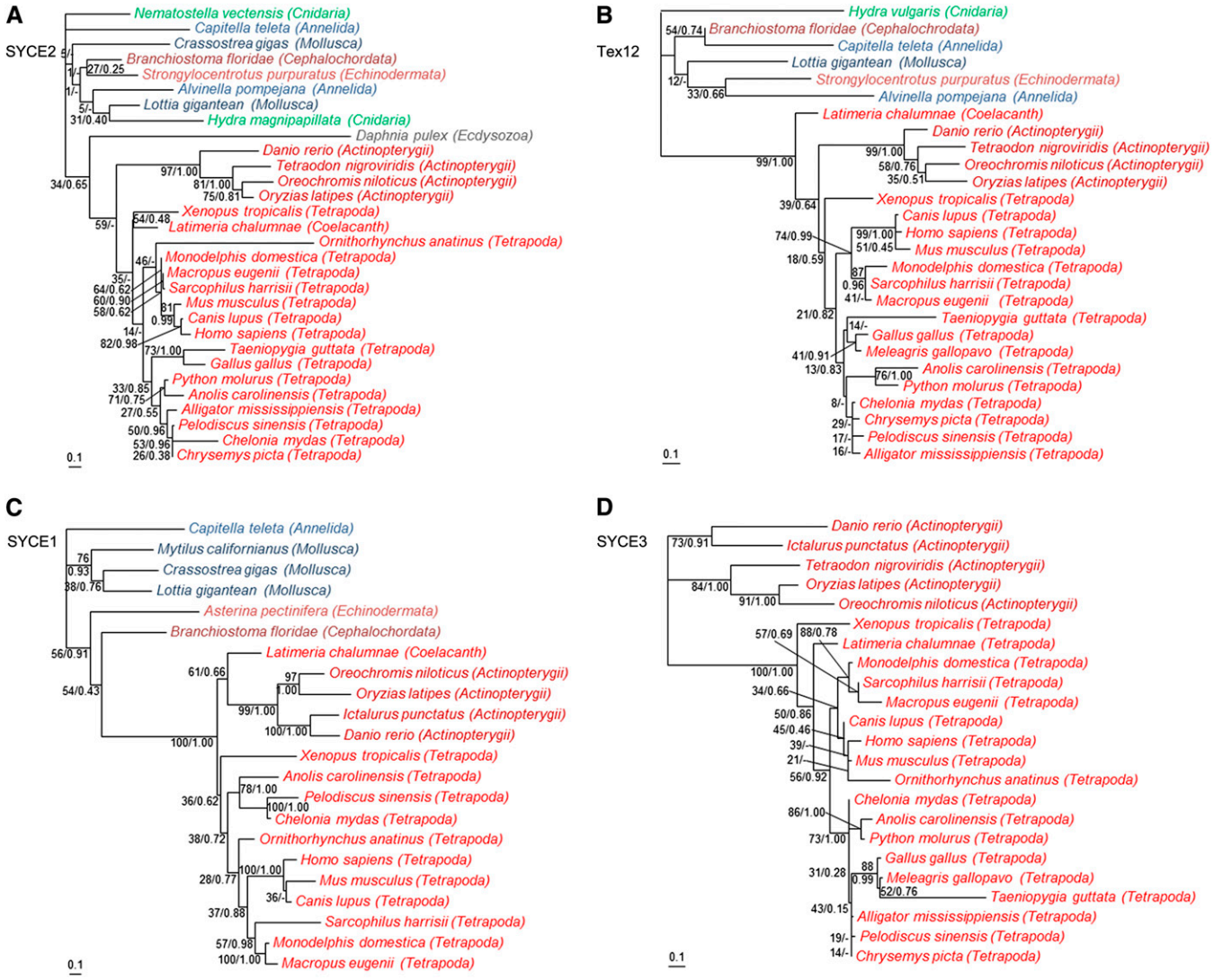

Figure 3 Unrooted maximum likelihood phylogenies of CE proteins. (A) SYCE2 (30 sequences, 75 aa positions kept). (B) Tex12 (27 sequences, 59 aa positions kept). (C) SYCE1 (22 sequences, 150 aa positions kept). (D) SYCE3 (23 sequences, 81 aa positions kept). Numbers at branches correspond to bootstrap values (given in percentages) and posterior probabilities (given in fractions) inferred with PhyML and MrBayes, respectively (e.g. 100/1.00). A dash indicates that the corresponding branch is not recovered in the consensus Bayesian tree (e.g. 46/-). Bars, average number of substitutions per site. Color code: *Cnidaria*, green; *Lophotrochozoa*, blue; *Ecdysozoa*, gray; and *Deuterostomia*, red. Sublineages are indicated by different shades of the same color.

conserved within the genus of *Drosophila* (Page *et al.* 2008). Consistently, we did not find homologous sequences beyond the border of this group using CONA as an alternative seed for our phylogenetic analysis.

A similar situation was reported in *C. elegans*. In total, four different SYP proteins (SYP-1, SYP-2, SYP-3, and SYP-4) have been identified to localize in the CR of the SC (MacQueen *et al.* 2002; Colaiacovo *et al.* 2003; Smolikov *et al.* 2007, 2009; Schild-Prüfert *et al.* 2011). However, it is yet unclear which proteins fulfill CE-like functions (Smolikov *et al.* 2009). According to the model proposed by Schild-Prüfert *et al.* (2011) SYP-1, which forms homodimers (or higher ordered structures), is most likely to be an essential module of the TFs (Schild-Prüfert *et al.* 2011) and was not included in the analysis. Using SYP-2, SYP-3, and SYP-4 as seeds for a homology search, we did not detect any homolog outside the genus *Caenorhabiditis*.

Expression of SYCE2 and TEX12 in Hydra meiosis

The presence of SYCE2 and Tex12 in *Cnidaria* and *Bilateria* indicates that they were present in their last common ancestor, *i.e.*, the *Eumetazoa* ancestor. Under the assumption that these proteins have not undergone functional changes, the cnidarian SYCE2 and Tex12 homologs are expected to be part of a SC in these animals. The competing hypothesis is that the SC is of more recent origin, but could have been built by the recruitment of ancient preexisting proteins. In this case, the cnidarian SYCE2 and Tex12 homologs should be involved in other functions. To discriminate between these two hypotheses, we tested the potential meiotic role

of the putative SYCE2 and Tex12 homologs in *H. vulgaris* (strain *AEP*). We first cloned and sequenced the putative full-length cDNA of *Hydra Syce2* (GenBank: KC580661) and *Tex12* (GenBank: KC580662) and subsequently performed an expression analysis on the level of mRNA as well as on the protein level. We applied RT–PCR on isolated mRNA from four different tissue fractions of *Hydra*—head, midpiece, foot, and testis—and could selectively amplify *Hydra Syce2* and *Tex12* cDNA in the testis fraction by using sequence-specific primers. A weak signal was also observed in the midpiece lane for *HySyce2*. This is not surprising, as *Hydra* testes grow as conical swellings along the body column and testis leftovers might have remained at the midpiece tissue during preparation. Amplification of *Hydra actin* served as an internal control for RT–PCR (Figure 4, A and B). By whole-mount *in situ* hybridization with DIG-labeled RNA probes that were complementary to the mRNAs of *Hydra Syce2* and *Tex12*, we could localize the transcripts to the basal cell layer of the conical testes of *Hydra* (Figure 4, C and D). In accordance with our findings, previous histological analysis of *Hydra* testis identified this region to be the location of spermatocytes (Kuznetsov *et al.* 2001).

In an approach similar to RT–PCR, we could also detect the corresponding protein product of Hy*Syce2* in the testis tissue by applying Western blot analysis. A specific and strong protein band of the predicted molecular mass of *Hydra* SYCE2 (17.6 kDa) appeared in the testis lane. Here as well, with the α-SYCE2 antibody, a faint protein band was also detected in the midpiece fraction (Figure 5). The raised α-Tex12 antibody was not effective in Western blot analysis.

Although the Hy*Tex12* protein product could not be detected by Western blot, the results indicated that *Hydra Syce2* and *Tex12* indeed are selectively expressed in meiotic cells, consistent with a role in *Hydra* meiosis. More detailed information about the localization of *Hydra* SYCE2 and Tex12 proteins was finally obtained by immunofluorescence analysis. The antibodies raised against the putative CE proteins were tested on chromosome spread preparations of *Hydra* testis tissue in at least two independent immunofluorescence experiments with a minimum of three slides. The resulting images of Figure 6 provide a representative picture of the observations in the confocal laser scanning microscope. As expected, the antibodies stained 15 SCs of *Hydra* pachytene spermatocytes that correlate in number to the quantity of homologous chromosome pairs in *H. vulgaris* (Zacharias *et al.* 2004). Colocalization of HySYCE2 and HySYCP1—a marker protein for the CR of the SC (Fraune *et al.* 2012b)—showed that the localization of the proteins fully overlap, but HySYCE2 exhibited a more punctate pattern than HySYCP1 along the synapsed SC in pachytene spermatocytes (Figure 6A). In contrast, HySYCE2 and HySYCP3—a marker protein for the chromosome axes (Fraune *et al.* 2012b)—only colocalize in regions where the chromosomes are synapsed via the CR. On unsynapsed axes in early diplotene, only HySYCP3 can be detected (Figure 6B, insets). Similar results were obtained for HyTex12, as its antibody worked effectively in immunofluorescence analysis. HyTex12 colocalized with HySYCP1 in pachytene spermatocytes (Figure 6C), but disappeared from the chromosome axes—marked by HySYCP3—in diplotene at sites where the SC disassembles and the chromosome axes become unsynapsed across long sections (Figure 6D, insets). At sites where the SC-mediated connection of the chromosome axes starts loosening, remains of HyTex12 can also be detected to localize between the two parallel running axes (marked by HySYCP3) of the bivalents (Figure 6D). Finally, double-label immunofluorescence microscopy of HySYCE2 and HyTex12 in a pachytene spermatocyte confirmed the punctate colocalization pattern of the two proteins within the cnidarian SC (Figure 6E).

Comparing our findings on the localization pattern of *Hydra* SYCE2 and Tex12 with the organization of the mammalian SC, both proteins obviously are cnidarian SC components specific to the CR. These results, therefore, strongly support the hypothesis of an ancestral SC in the ancestor of *Eumetazoa* formed by at least HySYCP1, HySYCP3 (Fraune *et al.* 2012b), as well as HySYCE2 and HyTex12.

Discussion

The evolutionary origin of mammalian CE-specific proteins of the SC

Our phylogenetic analyses indicate that three of the four mouse CE proteins appear to be conserved in the majority of metazoan clades. Especially homologs of SYCE2 and Tex12 could be traced back to the ancestor of *Eumetazoa*. Although we could not detect any homologous sequences in the oldest phyla of *Porifera* and *Placozoa*, we assume that these two proteins evolved at the time of metazoan origin. Our previously reported results, which described such an early origin of the main structural SC components SYCP1 and SYCP3 (Fraune *et al.* 2012b), support this assumption.

Our experimental data proved that *Hydra* SYCE2 and Tex12, in fact, are components of the cnidarian SC. The expression analysis demonstrated clearly the testis-specific synthesis of *Hydra* SYCE2 and Tex12. Antibodies raised against the proteins recognized SCs in *Hydra* spermatocytes. The punctate colocalization pattern of *Hydra* SYCE2 and Tex12 and their restriction to synapsed regions of the chromosome axes are therefore consistent with what is known from their mammalian homologs. In mouse, SYCE2 and Tex12 specifically localize to CE in a discontinuous pattern forming the so-called elongation complex that is responsible for the extension of synapsis along the entire chromosome length (Costa *et al.* 2005; Hamer *et al.* 2006, 2008; Bolcun-Filas *et al.* 2007). Recently, it was also reported that human SYCE2 and Tex12 form very stable and constitutive complexes under different experimental conditions. The regions located from aa 57 to 165 of human SYCE2 and 49 to 123 of human Tex12 were defined as essential for the capability to polymerize (Davies *et al.* 2012) and nicely correspond to the most conserved parts of the proteins in our analysis (Figure 1 and

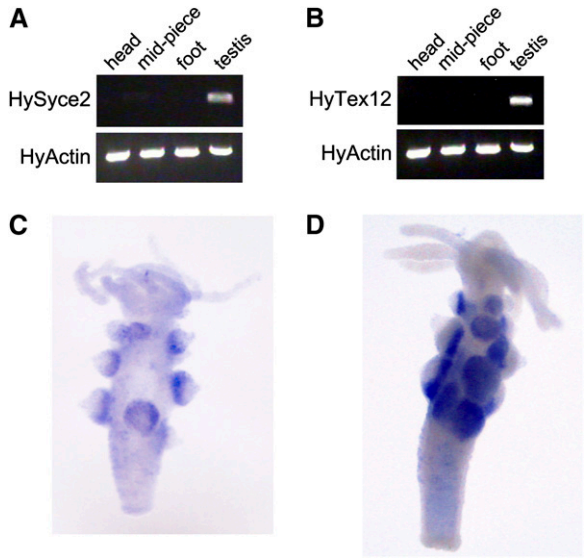

Figure 4 Expression analysis of *HySyce2* and *HyTex12*. Testis-specific synthesis of *HySyce2* (A) and *HyTex12* (B) mRNA is shown by RT–PCR as well as by *in situ* hybridization (C and D).

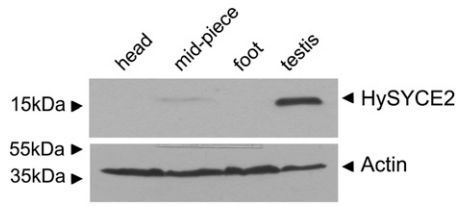

Figure 5 Protein expression of HySYCE2. HySYCE2 protein expression in the testis tissue is verified by immunoblotting.

Figure 2). It is therefore justified to assume that SYCE2 and Tex12 fulfill a similar function in the SC of different metazoans.

In mammals, SYCE1 and SYCE3 form the so-called initiation complex that, together with SYCP1, is involved in early synapsis steps between the axes of the homologous chromosomes. However, neither SYCE1 nor SYCE3 could be detected in *Hydra*. Homologs of SYCE1 were identified in different invertebrate clades including *Mollusca* and *Annelida*, suggesting an ancient origin, but an origin at the time of the rise of SYCE2 and Tex12 could not be demonstrated. This could be due to either too little sequence data or more likely to a true absence of SYCE1 homologs in nonbilaterian lineages. In contrast, SYCE3 is missing in all analyzed invertebrate genomes and therefore is most likely specific to the vertebrate lineage.

The picture that emerges from our analysis suggests that the mammalian SC is formed by very ancient (SYCE2, Tex12, and SYCE1) and much more recent elements (SYCE3). Although the structure of the SC is ancient in *Metazoa*, its composition has undergone a dynamic evolutionary history during the diversification of animals, which is summarized in the form of a model in Figure 7. The model illustrates the early origin of the *bona fide* structural SC proteins SYCP1 and SYCP3 (Fraune *et al.* 2012b) and of the elongation complex proteins SYCE2 and Tex12 in the ancestor of *Eumetazoa*. Further components were added step by step to the CE in the ancestor of *Bilateria* (SYCE1) and vertebrates (SYCE3). Finally, the absence of any SC protein homolog in *Nematoda* and *Hexapoda* also reflects the dynamic evolution of the SC and could be interpreted as either nonhomologous replacement of the ancestral components or their fast evolution beyond recognition (for further discussion, see section below).

The significance of the initiation complex and the elongation complex

Regarding the phylogenetic data, the elongation complex of the SC seems to be evolutionarily older than the initiation complex. However, our knowledge about the function of SYCE2/Tex12 and SYCE1/SYCE3 was obtained from investigations of only the mammalian proteins and their corresponding knockout mice. As the other available metazoan model systems for meiosis and the SC, *e.g.*, *D. melanogaster* and *C. elegans*, do not possess homologous CR proteins (see sections above and below), our present results provide a starting point for discussing the potential significance of the different CE components during evolution.

In previous polymerization studies using a heterologous system, it was shown that the mammalian TF protein SYCP1 is capable of self-assembling to higher ordered structures that resemble SCs, including the electron-dense region of the CE without support of any other SC protein (Öllinger *et al.* 2005). Beyond this, SYCP1 is recruited to the chromosome axes in mice even in the absence of single CE proteins (Hamer *et al.* 2008; Bolcun-Filas *et al.* 2009; Schramm *et al.* 2011). However, homologous chromosomes fail to start synapsis in the *Syce1* and *Syce3* knockout mice (Bolcun-Filas *et al.* 2009; Schramm *et al.* 2011). The absence of SYCE1 and SYCE3 homologs in *Cnidaria* could imply that different mechanisms of synapsis initiation are at work in this early-diverging animal lineage. Whether SYCP1 alone would be sufficient to initiate synapsis *in vivo* has not been investigated. However, our results also suggest that synapsis takes place in the absence of a mammalian-like initiation complex in these species. In mammals, it has been shown that the protein SYCE2 of the elongation complex is able to bind to SYCP1 (Costa *et al.* 2005). Whether SYCE2 of the cnidarians can bind to SYCP1 is not known. A direct binding of the protein to the TFs in this clade, however, could provide an explanation for the occurrence of an elongated synapsis even in the absence of a mammalian-like initiation complex made of SYCE1 and SYCE3.

The fact that the elongation complex is evolutionarily more conserved than the initiation complex could further be related to the process of homologous recombination. Knockout mice of the characterized CR proteins revealed a tight interdependency between the recombination machinery that is highly conserved in evolution (Cole *et al.* 2010) and the assembly of the CR (for review, see Fraune *et al.* 2012a). It is

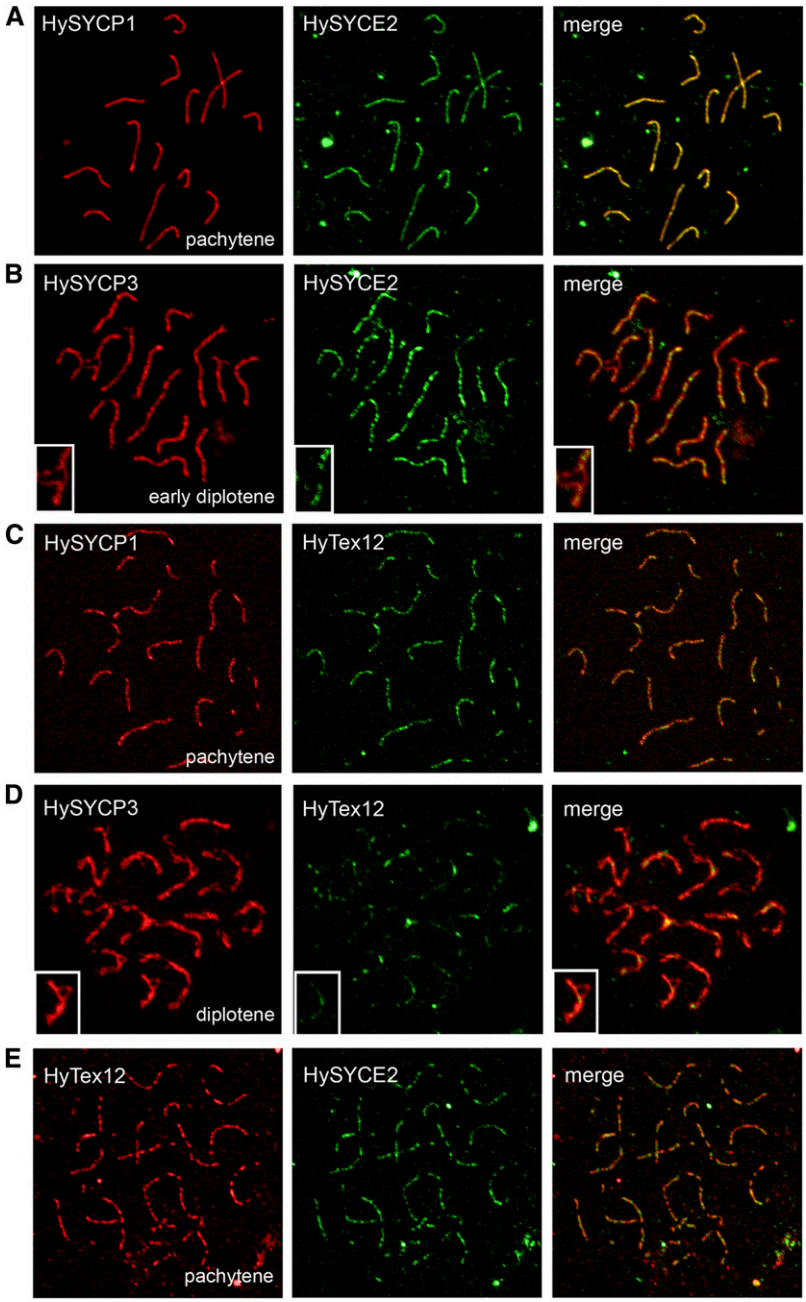

Figure 6 Immunolocalization of HySYCE2 and HyTex12 on chromosome spread preparations. HySYCE2 (A) and HyTex12 (C) colocalize with HySYCP1 to the fully synapsed chromosomes during pachytene, but exhibit a more punctate localization pattern. In early diplotene and diplotene, colocalization of HySYCE2 (B) and HyTex12 (D) with HySYCP3 is restricted to synapsed regions of the chromosomes. Double labeling of HySYCE2 and HyTex12 confirms their punctate colocalization pattern (E).

hypothesized that the CR might function as an essential platform for the recruitment of the recombination machinery to the chromosomes to generate crossovers, as close physical contacts between the CR and recombination nodules could be observed in the electron microscope (Schmekel and Daneholt 1998). In mammals, SYCP1 and SYCE2 were described to interact directly with RAD51, a RecA homolog responsible for the catalysis of the DNA strand exchange (Tarsounas *et al.* 1999; Moens *et al.* 2002; Bolcun-Filas *et al.* 2009), which reveals ~82% sequence identity between mouse (RefSeq: NP_035364.1) and *Hydra* (RefSeq: XP_002169171.1) (our unpublished data). If, together with SYCP1, SYCE2 is a linker protein between the CR and the homologous recombination machinery, it seems sensible that this protein and its tight interaction partner are conserved during metazoan evolution.

The evolutionary origin of alternative metazoan CE proteins

Considering the evolutionary trees of the metazoan CE proteins, the broad absence of ecdysozoan species is striking. As only SC components of *D. melanogaster* (CONA) and *C. elegans* (SYP-2, SYP-3, and SYP-4) are characterized from this clade (and invertebrates in general), these were the only starting options to explore the origin of these apparently nonhomologous CR proteins. Surprisingly, our search

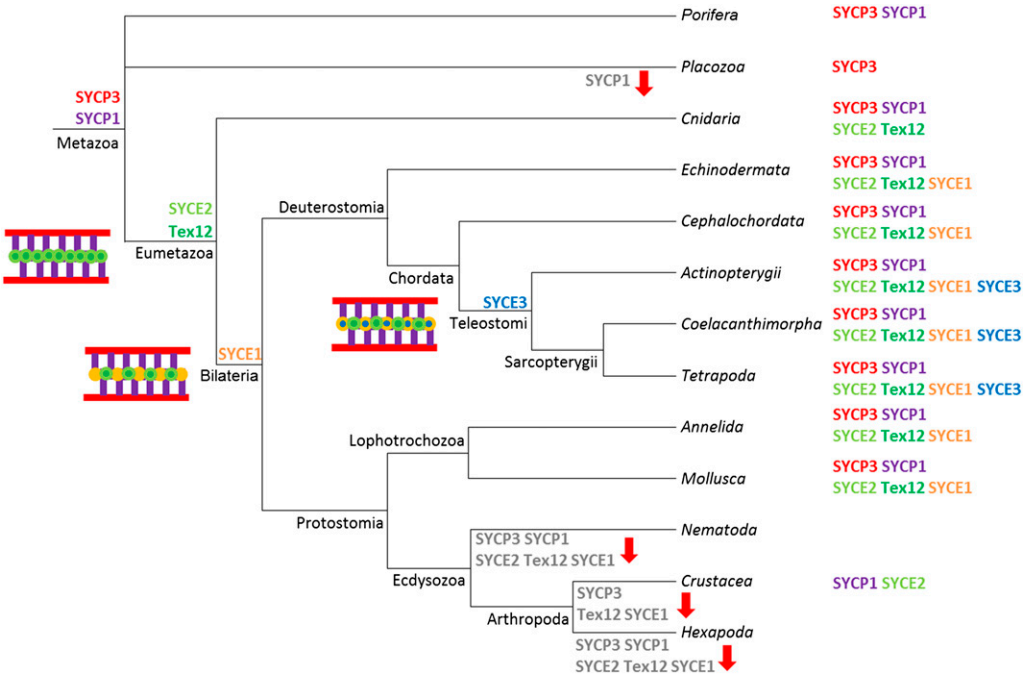

Figure 7 Model of the dynamic evolution of the SC in *Metazoa*. Given bioinformatic and experimental results of the preceding Fraune *et al.* (2012b) and the present study, the model shows that a basic SC of SYCP1, SYCP3, SYCE2, and Tex12 emerged in the last common ancestor of eumetazoan species. SYCE1 and SYCE3 evolved subsequently at the time of bilaterian and vertebrate emergence. Corresponding schematic illustrations of potential SC structures at the different evolutionary stages are shown. Homologs that were identified in the different taxonomic lineages of present-day organisms are listed next to the taxon name. Potential losses of homologs in certain lineages are indicated by the gray font of the respective protein names and a red arrow at the corresponding branch.

for homologs did not retrieve any sequences beyond the genus of either *Drosophila* or *Caenorhabditis*, pointing to the very recent and genus-specific origin of these proteins and asking the question about SC components being present in closely related lineages. As we could find neither any homologs that would bridge the sequence divergence between the mammalian CE proteins (or other mammalian proteins) nor any ecdysozoan CR protein, we are currently not in the position to make statements about the origin of these alternative CR proteins or their evolutionary relationship to the mammalian CE. However, two hypotheses may explain the available data: First, CONA of *D. melanogaster* and the SYP proteins of *C. elegans* are indeed nonhomologous proteins, but functional analogs to SYCE1, SYCE2, SYCE3, and/or Tex12, arisen independently by convergent evolution. The second hypothesis is that the CONA and SYP proteins derive from the CR proteins (SYCP1, SYCE1, SYCE2, and Tex12) that were present in the last common ancestor of *Bilateria*, but have diverged in the fast evolving *Ecdysozoa* to such a high degree that the homology is no longer recognizable. In fact, we favor the second hypothesis. The few crustacean sequences found in the case of SYCE2 (in this study) and SYCP1 (Fraune *et al.* 2012b) might be interpreted as an indicator for the existence of homologs in the ecdysozoan clade which, however, reveal a high evolutionary distance/divergence. A definitive answer, however, would require additional genomic and experimental data for these lineages.

Conclusion

We had previously demonstrated that the main structural components SYCP1 and SYCP3 of the mammalian SC are ancient in metazoans (Fraune *et al.* 2012b). Here, we show that this is also the case for three of the four proteins comprising the CE. Furthermore, we could clearly verify the testis-specific expression of the *Hydra* SYCE2 and Tex12 and showed that their localization pattern and dynamics in spermatocytes corresponds to that in mammals, pointing to a homology in sequence and conservation in function. Therefore, we conclude that not only the ladder-like structure of the SC, but also protein components of the three SC domains, namely, the LE (SYCP3), the TFs (SYCP1), and the CE (SYCE2 and Tex12) are conserved in *Metazoa* and presumably are indispensable for the basic functionality of the SC. The diversification of the main metazoan lineages was finally accompanied by a dynamic evolution of the SC, indicated by the nonhomologous replacement or the very fast divergence of some components in *Ecdysozoa* and the addition of further components in *Bilateria* (SYCE1) and vertebrates (SYCE3) (Figure 7).

Acknowledgments

We thank Jörg Schulz (Biocenter, University of Würzburg) for generous help at the beginning of this project, Thomas Bosch (University of Kiel) and his group for their support in issues regarding the culturing and treatment of *Hydra*, and Nicola Jones (Biocenter, University of Würzburg) for critical reading of the manuscript. J.F. and R.B. are supported by a grant of the Priority Program SPP1384: Mechanisms of genome haploidization (Deutsche Forschungsgemeinschaft). C.B-A. is supported by the Investissement d'Avenir grant (ANR-10-BINF-01-01) and is a member of the Institut Universitaire de France. The funders had no role in study design, data collection and analysis, decision to publish, or preparation of the manuscript.

Literature Cited

Altschul, S. F., T. L. Madden, A. A. Schaffer, J. Zhang, Z. Zhang *et al.*, 1997 Gapped BLAST and PSI-BLAST: a new generation of protein database search programs. Nucleic Acids Res. 25: 3389–3402.

Bolcun-Filas, E., and J. C. Schimenti, 2012 Genetics of meiosis and recombination in mice. Int Rev Cell Mol Biol 298: 179–227.

Bolcun-Filas, E., Y. Costa, R. Speed, M. Taggart, R. Benavente *et al.*, 2007 SYCE2 is required for synaptonemal complex assembly, double strand break repair, and homologous recombination. J. Cell Biol. 176: 741–747.

Bolcun-Filas, E., E. Hall, R. Speed, M. Taggart, C. Grey *et al.*, 2009 Mutation of the mouse *Syce1* gene disrupts synapsis and suggests a link between synaptonemal complex structural components and DNA repair. PLoS Genet. 5: e1000393.

Colaiacovo, M. P., A. J. MacQueen, E. Martinez-Perez, K. McDonald, A. Adamo *et al.*, 2003 Synaptonemal complex assembly in *C. elegans* is dispensable for loading strand-exchange proteins but critical for proper completion of recombination. Dev. Cell 5: 463–474.

Cole, F., S. Keeney, and M. Jasin, 2010 Evolutionary conservation of meiotic DSB proteins: more than just Spo11. Genes Dev. 24: 1201–1207.

Costa, Y., R. Speed, R. Öllinger, M. Alsheimer, C. A. Semple *et al.*, 2005 Two novel proteins recruited by synaptonemal complex protein 1 (SYCP1) are at the centre of meiosis. J. Cell Sci. 118: 2755–2762.

Costa, Y., and H. J. Cooke, 2007 Dissecting the mammalian synaptonemal complex using targeted mutations. Chromosome Res. 15: 579–589.

Criscuolo, A., and S. Gribaldo, 2010 BMGE (Block Mapping and Gathering with Entropy): a new software for selection of phylogenetic informative regions from multiple sequence alignments. BMC Evol. Biol. 10: 210.

Davies, O. R., J. D. Maman, and L. Pellegrini, 2012 Structural analysis of the human SYCE2–TEX12 complex provides molecular insights into synaptonemal complex assembly. Open Biol 2: 120099.

de Boer, E., F. G. Lhuissier, and C. Heyting, 2009 Cytological analysis of interference in mouse meiosis. Methods Mol. Biol. 558: 355–382.

Fraune, J., S. Schramm, M. Alsheimer, and R. Benavente, 2012a The mammalian synaptonemal complex: protein components, assembly and role in meiotic recombination. Exp. Cell Res. 318: 1340–1346.

Fraune, J., M. Alsheimer, J. N. Volff, K. Busch, S. Fraune *et al.*, 2012b *Hydra* meiosis reveals unexpected conservation of structural synaptonemal complex proteins across metazoans. Proc. Natl. Acad. Sci. USA 109: 16588–16593.

Gillies, C. B., 1975 Synaptonemal complex and chromosome structure. Annu. Rev. Genet. 9: 91–109.

Goodstadt, L., and C. P. Ponting, 2001 CHROMA: consensus-based colouring of multiple alignments for publication. Bioinformatics 17: 845–846.

Gouy, M., S. Guindon, and O. Gascuel, 2010 SeaView version 4: a multiplatform graphical user interface for sequence alignment and phylogenetic tree building. Mol. Biol. Evol. 27: 221–224.

Grens, A., L. Gee, D. A. Fisher, and H. R. Bode, 1996 *CnNK-2*, an *NK-2* homeobox gene, has a role in patterning the basal end of the axis in *Hydra*. Dev. Biol. 180: 473–488.

Guindon, S., J. Dufayard, V. Lefort, M. Anisimova, W. Hordijk *et al.*, 2010 New algorithms and methods to estimate maximum-likelihood phylogenies: assessing the performance of PhyML 3.0. Syst. Biol. 59: 307–321.

Hamer, G., K. Gell, A. Kouznetsova, I. Novak, R. Benavente *et al.*, 2006 Characterization of a novel meiosis-specific protein within the central element of the synaptonemal complex. J. Cell Sci. 119: 4025–4032.

Hamer, G., H. Wang, E. Bolcun-Filas, H. J. Cooke, R. Benavente *et al.*, 2008 Progression of meiotic recombination requires structural maturation of the central element of the synaptonemal complex. J. Cell Sci. 121: 2445–2451.

Handel, M. A., and J. C. Schimenti, 2010 Genetics of mammalian meiosis: regulation, dynamics and impact on fertility. Nat. Rev. Genet. 11: 124–136.

Hassold, T., and P. Hunt, 2001 To err (meiotically) is human: the genesis of human aneuploidy. Nat. Rev. Genet. 2: 280–291.

Hemmrich, G., K. Khalturin, A. M. Boehm, M. Puchert, F. Anton-Erxleben *et al.*, 2012 Molecular signatures of the three stem cell lineages in *Hydra* and the emergence of stem cell function at the base of multicellularity. Mol. Biol. Evol. 29: 3267–3280.

Jobb, G., A. von Haeseler, and K. Strimmer, 2004 TREEFINDER: a powerful graphical analysis environment for molecular phylogenetics. BMC Evol. Biol. 4: 18.

Katoh, K., K. Misawa, K.-I. Kuma, and T. Miyata, 2002 MAFFT: a novel method for rapid multiple sequence alignment based on fast Fourier transform. Nucleic Acids Res. 30: 3059–3066.

Kuznetsov, S., M. Lyanguzowa, and T. C. Bosch, 2001 Role of epithelial cells and programmed cell death in *Hydra* spermatogenesis. Zoology 104: 25–31.

Lammers, J. H., H. H. Offenberg, M. van Aalderen, A. C. Vink, A. J. Dietrich *et al.*, 1994 The gene encoding a major component of the lateral elements of synaptonemal complexes of the rat is related to X-linked lymphocyte-regulated genes. Mol. Cell. Biol. 14: 1137–1146.

Le, S. Q., and O. Gascuel, 2008 An improved general amino acid replacement matrix. Mol. Biol. Evol. 7: 1307–1320.

MacQueen, A. J., M. P. Colaiacovo, K. McDonald, and A. M. Villeneuve, 2002 Synapsis-dependent and -independent mechanisms stabilize homolog pairing during meiotic prophase in *C. elegans*. Genes Dev. 16: 2428–2442.

Martin, V. J., C. L. Littlefield, W. E. Archer, and H. R. Bode, 1997 Embryogenesis in *Hydra*. Biol. Bull. 192: 345–363.

Matsudaira, P., 1987 Sequence from picomole quantities of proteins electroblotted onto polyvinylidene difluoride membranes. J. Biol. Chem. 262: 10035–10038.

Meuwissen, R. L., H. H. Offenberg, A. J. Dietrich, A. Riesewijk, M. van Iersel *et al.*, 1992 A coiled-coil related protein specific for synapsed regions of meiotic prophase chromosomes. EMBO J. 11: 5091–5100.

Moens, P. B., N. K. Kolas, M. Tarsounas, E. Marcon, P. E. Cohen *et al.*, 2002 The time course and chromosomal localization of recombination-related proteins at meiosis in the mouse are compatible with models that can resolve the early DNA-DNA interactions without reciprocal recombination. J. Cell Sci. 115: 1611–1622.

Offenberg, H. H., J. A. Schalk, R. L. Meuwissen, M. van Aalderen, H. A. Kester *et al.*, 1998 SCP2: a major protein component of the axial elements of synaptonemal complexes of the rat. Nucleic Acids Res. 26: 2572–2579.

Öllinger, R., M. Alsheimer, and R. Benavente, 2005 Mammalian protein SCP1 forms synaptonemal complex-like structures in the absence of meiotic chromosomes. Mol. Biol. Cell 16: 212–217.

Ostlund, G., T. Schmitt, K. Forslund, T. Kostler, D. N. Messina *et al.*, 2010 InParanoid 7: New algorithms and tools for eukaryotic orthology analysis. Nucleic Acids Res. 38: D196–203.

Page, S. L., and R. S. Hawley, 2004 The genetics and molecular biology of the synaptonemal complex. Annu. Rev. Cell Dev. Biol. 20: 525–558.

Page, S. L., R. S. Khetani, C. M. Lake, R. J. Nielsen, J. K. Jeffress *et al.*, 2008 Corona is required for higher-order assembly of transverse filaments into full-length synaptonemal complex in *Drosophila* oocytes. PLoS Genet. 4: e1000194.

Philippe, H., R. Derelle, P. Lopez, K. Pick, C. Borchiellini *et al.*, 2009 Phylogenomics revives traditional views on deep animal relationships. Curr. Biol. 19: 706–712.

Ronquist, F., M. Teslenko, P. van der Mark, D. L. Ayres, A. Darling *et al.*, 2012 MrBayes 3.2: efficient bayesian phylogenetic inference and model choice across a large model space. Syst. Biol. 61: 539–542.

Schild-Prüfert, K., T. T. Saito, S. Smolikov, Y. Gu, M. Hincapie *et al.*, 2011 Organization of the synaptonemal complex during meiosis in *Caenorhabditis elegans*. Genetics 189: 411–421.

Schmekel, K., and B. Daneholt, 1998 Evidence for close contact between recombination nodules and the central element of the synaptonemal complex. Chromosome Res. 6: 155–159.

Schramm, S., J. Fraune, R. Naumann, A. Hernandez-Hernandez, C. Hoog *et al.*, 2011 A novel mouse synaptonemal complex protein is essential for loading of central element proteins, recombination, and fertility. PLoS Genet. 7: e1002088.

Sievers, F., A. Wilm, D. Dineen, T. J. Gibson, K. Karplus *et al.*, 2011 Fast, scalable generation of high-quality protein multiple sequence alignments using clustal omega. Mol. Syst. Biol. 7: 539.

Simakov, O., F. Marletaz, S. J. Cho, E. Edsinger-Gonzales, P. Havlak *et al.*, 2013 Insights into bilaterian evolution from three spiralian genomes. Nature 493: 526–531.

Smolikov, S., A. Eizinger, K. Schild-Prüfert, A. Hurlburt, K. McDonald *et al.*, 2007 SYP-3 restricts synaptonemal complex assembly to bridge paired chromosome axes during meiosis in *Caenorhabditis elegans*. Genetics 176: 2015–2025.

Smolikov, S., K. Schild-Prüfert, and M. P. Colaiacovo, 2009 A yeast two-hybrid screen for SYP-3 interactors identifies SYP-4, a component required for synaptonemal complex assembly and chiasma formation in *Caenorhabditis elegans* meiosis. PLoS Genet. 5: e1000669.

Tarsounas, M., T. Morita, R. E. Pearlman, and P. B. Moens, 1999 RAD51 and DMC1 form mixed complexes associated with mouse meiotic chromosome cores and synaptonemal complexes. J. Cell Biol. 147: 207–220.

von Wettstein, D., S. W. Rasmussen, and P. B. Holm, 1984 The synaptonemal complex in genetic segregation. Annu. Rev. Genet. 18: 331–411.

Wittlieb, J., K. Khalturin, J. U. Lohmann, F. Anton-Erxleben, and T. C. Bosch, 2006 Transgenic *Hydra* allow in vivo tracking of individual stem cells during morphogenesis. Proc. Natl. Acad. Sci. USA 103: 6208–6211.

Zacharias, H., B. Anokhin, K. Khalturin, and T. C. Bosch, 2004 Genome sizes and chromosomes in the basal metazoan *Hydra*. Zoology 107: 219–227.

Communicating editor: N. Hollingsworth

GENETICS

Supporting Information
http://www.genetics.org/lookup/suppl/doi:10.1534/genetics.113.156679/-/DC1

Phylogenies of Central Element Proteins Reveal the Dynamic Evolutionary History of the Mammalian Synaptonemal Complex: Ancient and Recent Components

Johanna Fraune, Céline Brochier-Armanet, Manfred Alsheimer, and Ricardo Benavente

DOI: 10.1534/genetics.113.156679

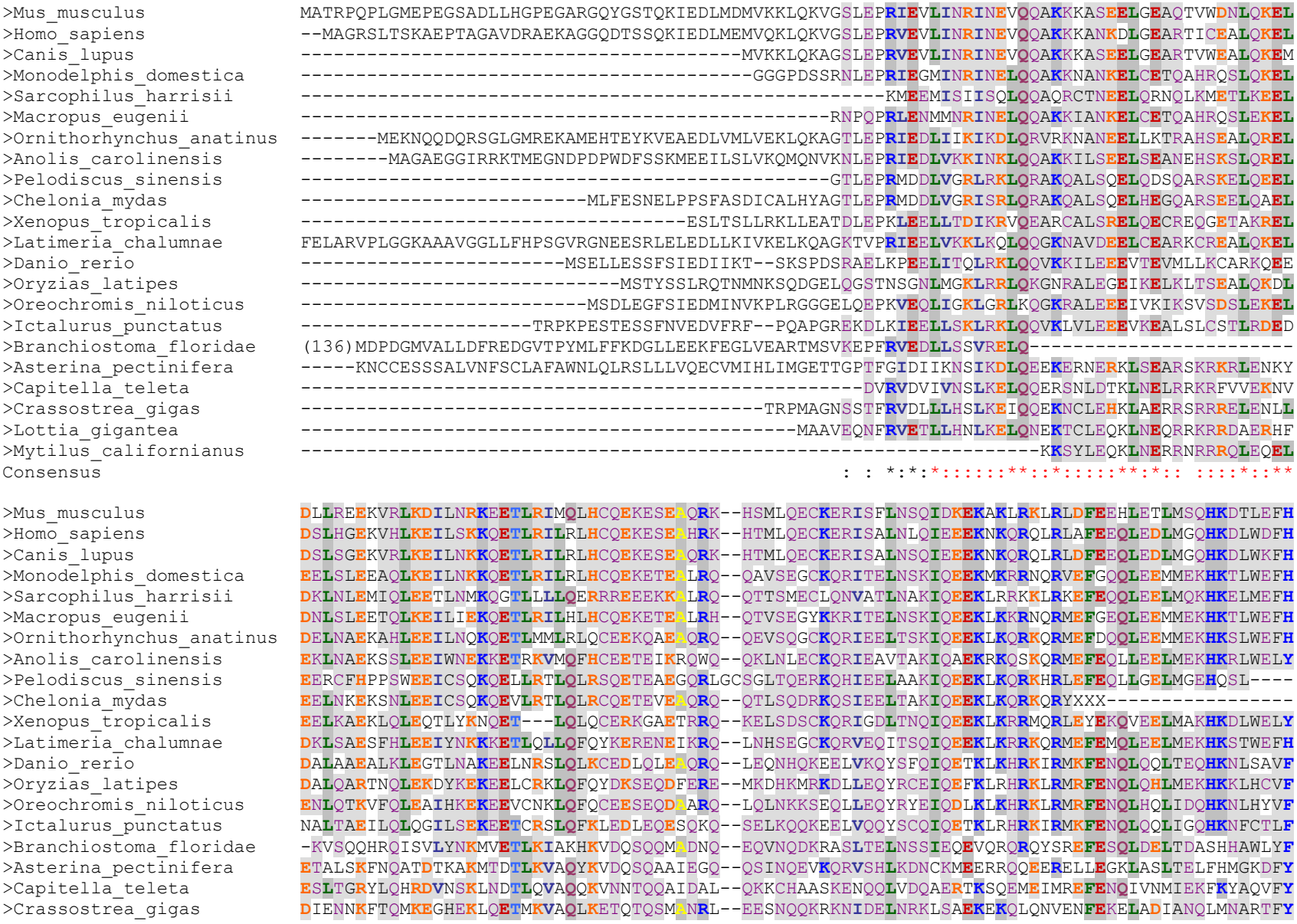
>Mus_musculus
>Homo_sapiens
>Canis_lupus
>Monodelphis_domestica
>Sarcophilus_harrisii
>Macropus_eugenii
>Ornithorhynchus_anatinus
>Anolis_carolinensis
>Pelodiscus_sinensis
>Chelonia_mydas
>Xenopus_tropicalis
>Latimeria_chalumnae
>Danio_rerio
>Oryzias_latipes
>Oreochromis_niloticus
>Ictalurus_punctatus
>Branchiostoma_floridae
>Asterina_pectinifera
>Capitella_teleta
>Crassostrea_gigas
>Lottia_gigantea
>Mytilus_californianus
Consensus

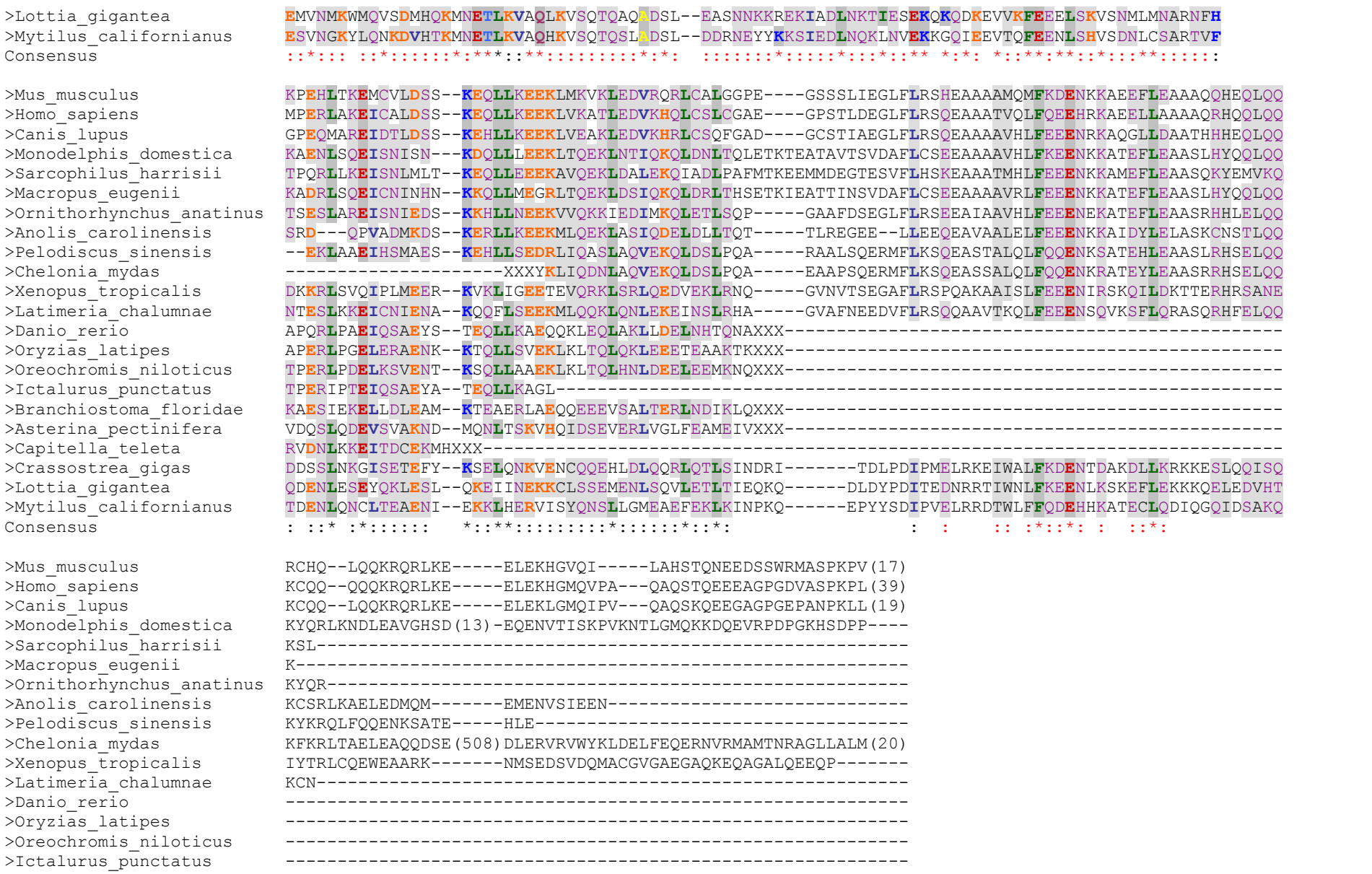
>Lottia_gigantea
>Mytilus_californianus
Consensus
>Mus_musculus
>Homo_sapiens
>Canis_lupus
>Monodelphis_domestica
>Sarcophilus_harrisii
>Macropus_eugenii
>Ornithorhynchus_anatinus
>Anolis_carolinensis
>Pelodiscus_sinensis
>Chelonia_mydas
>Xenopus_tropicalis
>Latimeria_chalumnae
>Danio_rerio
>Oryzias_latipes
>Oreochromis_niloticus
>Ictalurus_punctatus
>Branchiostoma_floridae
>Asterina_pectinifera
>Capitella_teleta
>Crassostrea_gigas
>Lottia_gigantea
>Mytilus_californianus
Consensus
>Mus_musculus
>Homo_sapiens
>Canis_lupus
>Monodelphis_domestica
>Sarcophilus_harrisii
>Macropus_eugenii
>Ornithorhynchus_anatinus
>Anolis_carolinensis
>Pelodiscus_sinensis
>Chelonia_mydas
>Xenopus_tropicalis
>Latimeria_chalumnae
>Danio_rerio
>Oryzias_latipes
>Oreochromis_niloticus
>Ictalurus_punctatus

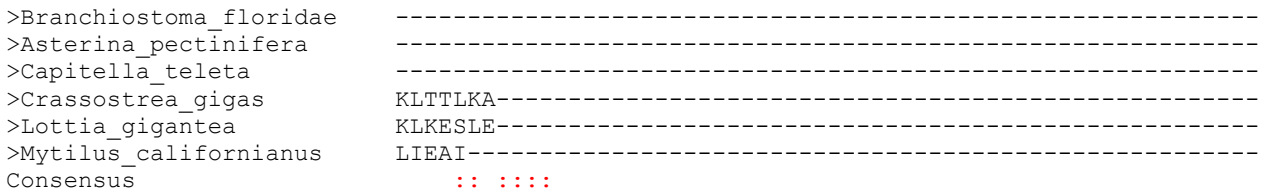

Figure S1 Multiple alignment of SYCE1 homologues. Positions kept for phylogenetic inferences are indicated in red.

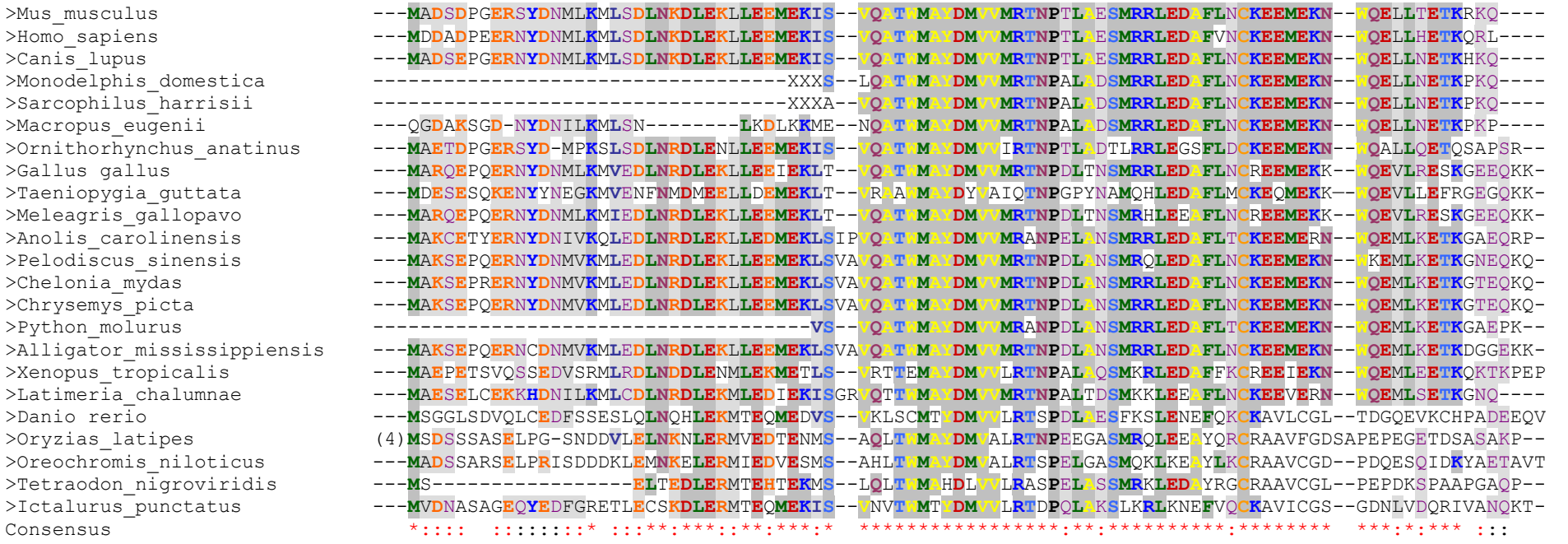
>Mus_musculus
>Homo_sapiens
>Canis_lupus
>Monodelphis_domestica
>Sarcophilus_harrisii
>Macropus_eugenii
>Ornithorhynchus_anatinus
>Gallus gallus
>Taeniopygia_guttata
>Meleagris_gallopavo
>Anolis_carolinensis
>Pelodiscus_sinensis
>Chelonia_mydas
>Chrysemys_picta
>Python_molurus
>Alligator_mississippiensis
>Xenopus_tropicalis
>Latimeria_chalumnae
>Danio rerio
>Oryzias_latipes
>Oreochromis_niloticus
>Tetraodon_nigroviridis
>Ictalurus_punctatus
Consensus
>Mus_musculus
>Homo_sapiens
>Canis_lupus
>Monodelphis_domestica
>Sarcophilus_harrisii
>Macropus_eugenii
>Ornithorhynchus_anatinus
>Gallus gallus
>Taeniopygia_guttata
>Meleagris_gallopavo
>Anolis_carolinensis
>Pelodiscus_sinensis
>Chelonia_mydas
>Chrysemys_picta
>Python_molurus
>Alligator_mississippiensis
>Xenopus_tropicalis
>Latimeria_chalumnae
>Danio rerio

```
>Oryzias_latipes                --TEM
>Oreochromis_niloticus          TLSQM
>Tetraodon_nigroviridis         ----D
>Ictalurus_punctatus            --TQE
Consensus
```

Figure S2 Multiple alignment of SYCE3 homologues. Positions kept for phylogenetic inferences are indicated in red.

Table S1 Origin of the SYCE2 homologues

Species name	Taxonomic rank	Accession number	sequence	Method/database	seed	E-value
M. musculus	Tetrapoda	NP_082230	complete	BLASTp/ *NCBI* nr		0
P. paniscus	Tetrapoda	XP_003814885	complete	BLASTp /*NCBI* nr	*M. musculus*	1e-70
R. norvegicus	Tetrapoda	EDL92193	complete	BLASTp /*NCBI* nr	*M. musculus*	5e-123
H. sapiens	Tetrapoda	NP_001099048	complete	BLASTp /*NCBI* nr	*M. musculus*	1e-70
P. troglodytes	Tetrapoda	XP_001155819	complete	BLASTp /*NCBI* nr	*M. musculus*	1e-70
P. abelii	Tetrapoda	XP_002828793	complete	BLASTp /*NCBI* nr	*M. musculus*	4e-71
P. anubis	Tetrapoda	XP_003915053	complete	BLASTp /*NCBI* nr	*M. musculus*	5e-70
N. leucogenys	Tetrapoda	XP_003256956	complete	BLASTp /*NCBI* nr	*M. musculus*	2e-70
L. africana	Tetrapoda	XP_003413389	complete	BLASTp /*NCBI* nr	*M. musculus*	8e-75
S. boliviensis	Tetrapoda	XP_003941778	complete	BLASTp /*NCBI* nr	*M. musculus*	2e-69
C. jacchus	Tetrapoda	XP_002761833	complete	BLASTp /*NCBI* nr	*M. musculus*	1e-66
C. lupus	Tetrapoda	XP_542039	complete	BLASTp /*NCBI* nr	*M. musculus*	2e-73
B. taurus	Tetrapoda	DAA28039	complete	BLASTp /*NCBI* nr	*M. musculus*	4e-74
M. mulatta	Tetrapoda	XP_002801138	complete	BLASTp /*NCBI* nr	*M. musculus*	1e-54
C. porcellus	Tetrapoda	XP_003468209	complete	BLASTp /*NCBI* nr	*M. musculus*	7e-58

O. cuniculus	Tetrapoda	XP_002724280	complete	BLASTp /*NCBI* nr	*M. usculus*	1e-64
S. scrofa	Tetrapoda	XP_003480827	complete	BLASTp /*NCBI* nr	*M. musculus*	4e-63
C. griseus	Tetrapoda	EGW00612	partial	BLASTp /*NCBI* nr	*M. musculus*	2e-45
A. melanoleuca	Tetrapoda	EFB28619	Complete	BLASTp /*NCBI* nr	*M. musculus*	4e-65
M. putorius	Tetrapoda	AES07688	Complete	BLASTp /*NCBI* nr	*M. musculus*	2e-64
O. garnettii	Tetrapoda	XP_003798068	partial	BLASTp /*NCBI* nr	*M. musculus*	1e-39
M. domestica	Tetrapoda	XP_001377747	complete	BLASTp /*NCBI* nr	*M. musculus*	6e-57
S. harrisii	Tetrapoda	XP_003760717	complete	BLASTp /*NCBI* nr	*M. musculus*	4e-56
M. eugenii	Tetrapoda	ABQO021047289	partial	tBLASTn/*NCBI* wgs	*S. harrisii*	3e-41
O. anatinus	Tetrapoda	ENSOANP00000014450	partial	BLASTp*/UniProtKB*	*M. musculus*	2x10-5
G. gallus	Tetrapoda	XP_003643433	complete	BLASTp /*NCBI* nr	*M. musculus*	1e-37
T. guttata	Tetrapoda	XP_002194928	partial	BLASTp /*NCBI* nr	*M. musculus*	4e-15
A. carolinensis	Tetrapoda	XP_003216437	complete	BLASTp /*NCBI* nr	*M. musculus*	6e-36
P. sinensis	Tetrapoda	ENSPSIP00000014147	partial	BLASTp/ *UniProtKB*	*A. carolinensis*	9x10-31
P. molurus	Tetrapoda	AEQU010394814	partial	tBLASTn/*NCBI* wgs	*A. carolinensis*	3e-30
A. mississippiensis	Tetrapoda	AKHW01024067	partial	tBLASTn/*NCBI* wgs	*A. carolinensis*	2e-18

C. mydas	Tetrapoda	EMP37242	complete	BLASTp /*NCBI* nr	*A. carolinensis*	3e-23
C. picta	Tetrapoda	AHGY01185898	partial	tBLASTn/*NCBI* wgs	*A. carolinsensis*	1e-21
X. tropicalis	Tetrapoda	XP_002939167	partial	BLASTp /*NCBI* nr	*M. musculus*	1e-19
L. chalumnae	Coelacanth	AFYH01158832	partial	tBLASTn/*NCBI* wgs	*A. carolinensis*	8e-17
D. rerio	Actinopterygii	NP_001018339	complete	BLASTp /*NCBI* nr	*M. musculus*	2e-11
O. mykiss	Actinopterygii	BX_298349	complete	tBLASTn/*Gene Indices*	*D. rerio*	1,6e-44
O. latipes	Actinopterygii	FS528043	complete	tBLASTn/*Gene Indices*	*D. rerio*	1,1e-22
O. niloticus	Actinopterygii	XP_003453800	complete	BLASTp /*NCBI* nr	*M. musculus*	2e-06
T.nigroviridis	Actinopterygii	CAG03308	complete	BLASTp /*NCBI* nr	*M. musculus*	6e-10
B. floridae	Cephalochordata	XP_002591412	complete	BLASTp /*NCBI* nr	*M. musculus*	8e-15
C. savignyi	Tunicata	BW516106	complete	tBLASTn/*NCBI* est	*H. diversicolor*	2e-09
C. intestinalis	Tunicata	XP_002130896	complete	BLASTp /*NCBI* nr	*M. musculus*	0,008
P. misakiensis	Tunicata	AU036426	complete	tBLASTn/*NCBI* est	*H. diversicolor*	2e-06
S. purpuratus	Echinodermata	XP_003726746	complete	BLASTp /*NCBI* nr	*M. musculus*	1e-13
A. pompejana	Annelida	GO169636	complete	tBLASTn/*NCBI* est	*L. gigantea*	2e-14
C. teleta	Annelida	Jgi 210482 AMQN01004103	complete	Blastp/l*nParanoid* tBLASTn/*NCBI* wgs	*M. musculus* *C. teleta*	4,9e-06

S. nudus	Annelida	FR768618	complete	tBLASTn/*NCBI* est	*L. gigantea*	2e-23
L. stagnalis	Mollusca	ES573602	complete	tBLASTn/*NCBI* est	*L. gigantea*	1e-09
L. gigantea	Mollusca	jgi 158004 AMQO01001743	complete	Blastp/I*nParanoid* tBLASTn/*NCBI* wgs	*M. musculus* *L. gigantea*	1,8e-08
C. gigas	Mollusca	EKC37702	complete	BLASTp /*NCBI* nr	*M. musculus*	1e-04
H. diversicolor	Mollusca	GT866818	complete	tBLASTn/*NCBI* est	*L. gigantea*	2e-32
D. pulex	Crustacea	EFX69051	complete	Hmmsearch/*NCBI* est	*hmmprofil*	0,023
H. magnipapillata	Cnidaria	XP_002165182	complete	BLASTp /*NCBI* nr	*M. musculus*	5e-06
N. vectensis	Cnidaria	XP_001625149	complete	BLASTp /*NCBI* nr	*M. musculus*	2e-11

Table S2 Origin of the Tex12 homologues

Species name	Taxonomic rank	Accession number	sequence	Method/database	seed	E-value
M. musculus	Tetrapoda	NP_079963	complete	BLASTp /*NCBI* nr		0
S. boliviensis	Tetrapoda	XP_003923759	complete	BLASTp /*NCBI* nr	*M. musculus*	2e-60
C. griseus	Tetrapoda	XP_003498567	complete	BLASTp /*NCBI* nr	*M. musculus*	2e-68
L. africana	Tetrapoda	XP_003415682	complete	BLASTp /*NCBI* nr	*M. musculus*	3e-63
B. taurus	Tetrapoda	NP_001029435	complete	BLASTp /*NCBI* nr	*M. musculus*	2e-63
M. mulatta	Tetrapoda	NP_001181321	complete	BLASTp /*NCBI* nr	*M. musculus*	1e-61
O. garnettii	Tetrapoda	XP_003794793	complete	BLASTp /*NCBI* nr	*M. musculus*	1e-59
O. cuniculus	Tetrapoda	XP_002708480	complete	BLASTp /*NCBI* nr	*M. musculus*	7e-64
E. caballus	Tetrapoda	XP_001501942	complete	BLASTp /*NCBI* nr	*M. musculus*	1e-63
P. abelii	Tetrapoda	XP_002822521	complete	BLASTp/*NCBI* nr	*M. musculus*	6e-62
H. sapiens	Tetrapoda	NP_112565	complete	BLASTp /*NCBI* nr	*M. musculus*	9e-62
A. melanoleuca	Tetrapoda	XP_002921152	complete	BLASTp /*NCBI* nr	*M. musculus*	5e-61
S. scrofa	Tetrapoda	XP_003357347	complete	BLASTp /*NCBI* nr	*M. musculus*	7e-63
C. porcellus	Tetrapoda	XP_003472874	complete	BLASTp /*NCBI* nr	*M. musculus*	2e-57
R. norvegicus	Tetrapoda	NP_001178035	complete	BLASTp /*NCBI* nr	*M. musculus*	1e-72

C. lupus	Tetrapoda	XP_854089	complete	BLASTp/*NCBI* nr	*M. musculus*	2e-64
H. glaber	Tetrapoda	EHB18703	complete	BLASTp /*NCBI* nr	*M. musculus*	7e-18
C. jacchus	Tetrapoda	XP_003734157	complete	BLASTp /*NCBI* nr	*M. musculus*	3e-37
S. harrisii	Tetrapoda	XP_003764283	complete	BLASTp /*NCBI* nr	*M. musculus*	1e-36
M. domestica	Tetrapoda	AAFR03009835	complete	tBLASTn/*NCBI* wsg	*S. harrisii*	2e-23
M. eugenii	Tetrapoda	ENSMEUP00000005950	partial	tBLASTn/*Ensembl genomic sequence*	*S. harrisii*	5.4e-59
M. gallopavo	Tetrapoda	XP_003212810	complete	BLASTp /*NCBI* nr	*M. musculus*	3e-29
G. gallus	Tetrapoda	XP_001233099	complete	BLASTp /*NCBI* nr	*M. musculus*	3e-27
T. guttata	Tetrapoda	ABQF01045735	partial	tBLASTn/*NCBI* wsg	*G. gallus*	7e-16
A. carolinensis	Tetrapoda	FG795025	complete	tBLASTn/*NCBI* est	*O. niloticus*	1e-06
P. sinensis	Tetrapoda	AGCU01007591	partial	tBLASTn/*NCBI* wsg	*A. carolinensis*	9e-12
P. molurus	Tetrapoda	AEQU010325864	partial	tBLASTn/*NCBI* wsg	*A. carolinensis*	2e-16
C. mydas	Tetrapoda	AJIM01191925	partial	tBLASTn/*NCBI* wsg	*A. carolinensis*	1e-12
C. picta	Tetrapoda	AHGY01090089	partial	tBLASTn/*NCBI* wsg	*A. carolinensis*	3e-12
A. mississippisiensis	Tetrapoda	AKHW01088812	partial	tBLASTn/*NCBI* wsg	*A. carolinensis*	1e-10
X. tropicalis	Tetrapoda	XP_002942798	complete	BLASTp /*NCBI* nr	*M. musculus*	5e-15

L. chalumnae	Coelacanth	BAHO01008061	partial	tBLASTn/*NCBI* wsg	*A. carolinensis*	8e-09
D. rerio	Actinopterygii	XP_003200088	complete	BLASTp /*NCBI* nr	*M. musculus*	2e-10
A. fimbria	Actinopterygii	ACQ58790	complete	BLASTp /*NCBI* nr	*M. musculus*	2e-08
O. niloticus	Actinopterygii	XP_003453604	complete	BLASTp /*NCBI* nr	*M. musculus*	0,21
O. latipes	Actinopterygii	FS551872	complete	tBLASTn/*NCBI* est	*O. niloticus*	4e-39
T. nigroviridis	Actinopterygii	CR716219	Complete	tBLASTn/*NCBI* nr	*O. niloticus*	5e-22
R. rutilus	Actinopterygii	EG548787	complete	tBLASTn/*NCBI* est	*O. niloticus*	1e-21
P. promelas	Actinopterygii	DT342891	complete	tBLASTn/*NCBI* est	*O. niloticus*	5e-21
D. labrax	Actinopterygii	FM002700	complete	tBLASTn/*NCBI* est	*O. niloticus*	1e-41
O. mykiss	Actinopterygii	CR370999	complete	tBLASTn/*NCBI* est	*O. niloticus*	1e-26
I. furcatus	Actinopterygii	FD158102	complete	tBLASTn/*NCBI* est	*O. niloticus*	6e-11
G. morhua	Actinopterygii	EY966699	complete	tBLASTn/*NCBI* est	*O. niloticus*	3e-20
P. olivaceus	Actinopterygii	CX286679	complete	tBLASTn/*NCBI* est	*O. niloticus*	3e-18
S. salar	Actinopterygii	CB508238	partial	tBLASTn/*NCBI* est	*O. niloticus*	2e-24
B. floridae	Cephalochordata	XP_002590156	complete	BLASTp /*NCBI* nr	*M. musculus*	0,15
S. purpuratus	Echinodermata	AAGJ04009105	partial	tBLASTn/*NCBI* wsg	*A. pompejana*	0,35

C. teleta	Annelida	AMQN01002974	partial	tBLASTn/*NCBI* wsg	*L. gigantea*	8e-05
A. pompejana	Annelida	GO142621	complete	tBLASTn/*NCBI* est	*G. gallus*	0,009
L. gigantea	Mollusca	AMQO01006439	complete	tBLASTn/*NCBI* wsg	*B. floridae*	2e-09
H. vulgaris	Cnidaria	CN567182	complete	tBLASTn/*NCBI* est	*B. floridae*	3e-09

Table S3 Origin of the SYCE1 homologues

Species name	Taxonomic rank	Accession number	sequence	Method/database	seed	E-value
M. musculus	Tetrapoda	NP_001137237	complete	BLASTp/*NCBI* nr		0
R. norvegicus	Tetrapoda	NP_001020229	complete	BLASTp /*NCBI* nr	*M. musculus*	0
H. sapiens	Tetrapoda	NP_001137236	complete	BLASTp/*NCBI* nr	*M. musculus*	7e-119
P. troglodytes	Tetrapoda	XP_001146521	complete	BLASTp /*NCBI* nr	*M. musculus*	1e-117
P. abelii	Tetrapoda	XP_002821352	complete	BLASTp /*NCBI* nr	*M. musculus*	1e-120
C. porcellus	Tetrapoda	XP_003479623	complete	BLASTp/*NCBI* nr	*M. musculus*	2e-144
N. leucogenys	Tetrapoda	XP_003275547	complete	BLASTp /*NCBI* nr	*M. musculus*	6e-117
P. paniscus	Tetrapoda	XP_003805584	complete	BLASTp /*NCBI* nr	*M. musculus*	2e-115
A. melanoleuca	Tetrapoda	XP_002928741	complete	BLASTp /*NCBI* nr	*M. musculus*	1e-138
C. griseus	Tetrapoda	XP_003514379	complete	BLASTp /*NCBI* nr	*M. musculus*	4e-169
L. africana	Tetrapoda	XP_003423552	complete	BLASTp /*NCBI* nr	*M. musculus*	3e-122
M. mulatta	Tetrapoda	XP_002805923	complete	BLASTp /*NCBI* nr	*M. musculus*	4e-116
E. caballus	Tetrapoda	XP_001497316	complete	BLASTp /*NCBI* nr	*M. musculus*	1e-126
P. anubis	Tetrapoda	XP_003904501	complete	BLASTp /*NCBI* nr	*M. musculus*	2e-120
O. cuniculus	Tetrapoda	XP_002718820	complete	BLASTp /*NCBI* nr	*M. musculus*	2e-123

B. taurus	Tetrapoda	NP_001033238	complete	BLASTp /*NCBI* nr	*M. musculus*	5e-128
C. lupus	Tetrapoda	XP_537943	complete	BLASTp /*NCBI* nr	*M. musculus*	4e-144
O. garnettii	Tetrapoda	XP_003803715	complete	BLASTp /*NCBI* nr	*M. musculus*	7e-140
M. fascicularis	Tetrapoda	Q4R7J8	complete	BLASTp /*NCBI* nr	*M. musculus*	3e-101
H. glaber	Tetrapoda	EHB13133	complete	BLASTp /*NCBI* nr	*M. musculus*	1e-94
M. domestica	Tetrapoda	ADB77889	complete	BLASTp /*NCBI* nr	*M. musculus*	4e-55
S. harrisii	Tetrapoda	ENSSHAP00000009845	partial	BLASTp /*UniProtKB*	*M. domestica*	1x10-52
M. eugenii	Tetrapoda	FY576800	complete	tBLASTn*/NCBI* est	*M. domestica*	7e-109
S. boliviensis	Tetrapoda	XP_003938136	complete	BLASTp /*NCBI* nr	*M. musculus*	3e-38
C. jacchus	Tetrapoda	XP_003735392	complete	BLASTp /*NCBI* nr	*M. musculus*	2e-39
O. anatinus	Tetrapoda	ENSOANP00000022990	complete	BLASTp*/ UniProtKB*	*M. domestica*	4x10-76
A. carolinensis	Tetrapoda	XP_003216702	complete	BLASTp /*NCBI* nr	*M. musculus*	5e-44
C. mydas	Tetrapoda	EMP26554	partial	BLASTp/*NCBI* nr	*A. carolinensis*	6e-33
P. sinensis	Tetrapoda	ENSPSIP00000010027	partial	BLASTp/*UniProtKB*	*A. carolinensis*	2x10-38
X. tropicalis	Tetrapoda	XP_002943661	complete	BLASTp /*NCBI* nr	*M. musculus*	3e-20
L. chalumnea	Coelacanth	H3ALY1	complete	Hmmsearch/*UniProt*	*hmmprofil*	8,7e-77

P. reticulata	Actinopterygii	ES386322	complete	tBLASTn/*NCBI* est	*O. latipes*	2e-49
R. rutilus	Actinopterygii	EG545611	complete	tBLASTn/*NCBI* est	*O. latipes*	3e-36
I. punctatus	Actinopterygii	CK426085	complete	tBLASTn/*NCBI* est	*O. latipes*	3e-31
P. promelas	Actinopterygii	DT113652	partial	tBLASTn/*NCBI* est	*O. latipes*	2e-23
S. maximus	Actinopterygii	HQ603845	partial	tBLASTn/*NCBI* est	*O. latipes*	3e-23
P. maniculatus	Actinopterygii	GH530402	complete	tBLASTn/*NCBI* est	*O. latipes*	3e-09
O. niloticus	Actinopterygii	XP_003444205	complete	BLASTp /*NCBI* nr	*M. musculus*	1e-17
D. rerio	Actinopterygii	XP_694355	complete	tBLASTn/*NCBI* est	*M. musculus*	5e-14
O. latipes	Actinopterygii	XP_004074263	complete	BLASTp/*NCBI* nr	*D. rerio*	1e-32
B. floridae	Cephalochordata	XP_002592847	complete	tBLASTn/*NCBI* nr	*O. latipes*	0,16
A. pectinifera	Echinodermata	DB424359	complete	tBLASTn/*NCBI* est	*L. gigantea*	1e-12
C. teleta	Annelida	AMQN01011277	complete	tBLASTn/*NCBI* wsg	*L. gigantea*	2e-12
M. californianus	Mollusca	ES407417	partial	tBLASTn/*NCBI* est	*B. floridae*	1e-10
L. gigantea	Mollusca	jgi 156257 AMQO01001205	complete	Blastp/*InParanoid* tBLASTn/*NCBI* wsg	*M. musculus* *L. gigantea*	<0,01
C. gigas	Mollusca	AM858590	complete	tBLASTn/*NCBI* est	*L. gigantea*	3e-48

Table S4 Origin of the SYCE3 homologues

Species name	Taxonomic rank	Accession number	sequence	Method/database	seed	E-value
M. musculus	Tetrapoda	NP_001156352	complete	BLASTp /*NCBI* nr		0
A. melanoleuca	Tetrapoda	XP_002917318	complete	BLASTp /*NCBI* nr	*M. musculus*	6e-57
C. porcellus	Tetrapoda	XP_003461608	complete	BLASTp /*NCBI* nr	*M. musculus*	1e-54
C. griseus	Tetrapoda	XP_003515506	complete	BLASTp /*NCBI* nr	*M. musculus*	5e-59
B. taurus	Tetrapoda	XP_001193262	complete	BLASTp /*NCBI* nr	*M. musculus*	2e-54
R. norvegicus	Tetrapoda	NP_001128725	complete	BLASTp /*NCBI* nr	*M. musculus*	3e-59
E. caballus	Tetrapoda	XP_003364377	complete	BLASTp /*NCBI* nr	*M. musculus*	8e-58
L. africana	Tetrapoda	XP_003423236	complete	BLASTp/*NCBI* nr	*M. musculus*	3e-46
S. scrofa	Tetrapoda	NP_001193291	complete	BLASTp /*NCBI* nr	*M. musculus*	9e-56
O. cuniculus	Tetrapoda	XP_002723272	complete	BLASTp /*NCBI* nr	*M. musculus*	4e-56
C. lupus	Tetrapoda	XP_003431525	complete	BLASTp /*NCBI* nr	*M. musculus*	7e-57
S. boliviensis	Tetrapoda	XP_003932838	complete	BLASTp /*NCBI* nr	*M. musculus*	7e-53
M. mulatta	Tetrapoda	NP_001180282	complete	BLASTp /*NCBI* nr	*M. musculus*	1e-53
O. garnettii	Tetrapoda	XP_003783125	complete	BLASTp /*NCBI* nr	*M. musculus*	3e-56
P. troglodytes	Tetrapoda	XP_001156556	complete	BLASTp /*NCBI* nr	*M. musculus*	2e-52

H. sapiens	Tetrapoda	NP_001116697	complete	BLASTp /*NCBI* nr	*M. musculus*	2e-52
O.anatinus	Tetrapoda	XP_003430278	complete	BLASTp /*NCBI* nr	*M. musculus*	2e-43
H. glaber	Tetrapoda	EHB03472	complete	BLASTp /*NCBI* nr	*M. musculus*	9e-50
N. leucogenys	Tetrapoda	XP_003281537	partial	BLASTp /*NCBI* nr	*M. musculus*	2e-28
M. domestica	Tetrapoda	XP_003341970	partial	BLASTp /*NCBI* nr	*M. musculus*	2e-28
S. harrisii	Tetrapoda	XP_003770860	partial	BLASTp /*NCBI* nr	*M. musculus*	2e-28
M. eugenii	Tetrapoda	ENSMEUP00000004105	partial	tBLASTn/*Ensembl genomic*	*S. harrisii*	1.2e-38
O. anatinus	Tetrapoda	XP_003430278	complete	BLASTp /*NCBI* nr	*G. gallus*	9e-35
G. gallus	Tetrapoda	XP_001231764	complete	BLASTp /*NCBI* nr	*M. musculus*	5e-44
T. guttata	Tetrapoda	XP_002188999	complete	BLASTp /*NCBI* nr	*M. musculus*	1e-24
M. gallopavo	Tetrapoda	XP_003202713	complete	BLASTp /*NCBI* nr	*M. musculus*	4e-43
A. carolinensis	Tetrapoda	AAWZ02027734	complete	tBLASTn/*NCBI* wsg	*G. gallus*	2e-24
P. sinensis	Tetrapoda	AGCU01015398 AGCU01015399	complete	tBLASTn/*NCBI* wsg	*A. carolinensis*	6e-26 4e-10
C. mydas	Tetrapoda	AJIM01252458	complete	tBLASTn/*NCBI* wsg	*G. gallus*	7e-33
C. picta	Tetrapoda	AHGY01153388	complete	tBLASTn/*NCBI* wsg	*G. gallus*	2e-31
P. molurus	Tetrapoda	AEQU010368279	partial	tBLASTn/*NCBI* wsg	*A. carolinensis*	1e-29

A. mississippisiensis	Tetrapoda	AKHW01109662	complete	tBLASTn/*NCBI* wsg	*A. carolinensis*	5e-28
X. tropicalis	Tetrapoda	XP_002939573	complete	BLASTp /*NCBI* nr	*M. musculus*	4e-32
L. chalumnea	Coelacanth	BAHO01390606	complete	tBLASTn/*NCBI* wsg	*A. carolinensis*	3e-20
D. rerio	Actinopterygii	NP_001129458	complete	BLASTp /*NCBI* nr	*M. musculus*	3e-12
O. niloticus	Actinopterygii	XP_003445882	complete	BLASTp /*NCBI* nr	*M. musculus*	3e-13
T. nigroviridis	Actinopterygii	CAG10121	partial	BLASTp /*NCBI* nr	*M. musculus*	3e-15
O. latipes	Actinopterygii	FS547734	complete	tBLASTn/*NCBI* est	*O. niloticus*	4e-34
P. flavescens	Actinopterygii	GO658805	complete	tBLASTn/*NCBI* est	*O. niloticus*	2e-33
H. hippoglossus	Actinopterygii	FD698650	complete	tBLASTn/*NCBI* est	*O. niloticus*	1e-20
R. rutilus	Actinopterygii	EG545621	complete	tBLASTn/*NCBI* est	*O. niloticus*	3e-17
I. punctatus	Actinopterygii	CK419473	complete	tBLASTn/*NCBI* est	*O. niloticus*	3e-17
T. thynnus	Actinopterygii	EG630239	partial	tBLASTn/*NCBI* est	*O. niloticus*	2e-16